MOMENT: A Family of Open Time-series Foundation Models

Mononito Goswami [1]   Konrad Szafer [*1]   Arjun Choudhry [*1]   Yifu Cai [1]   Shuo Li [2]   Artur Dubrawski [1]

Abstract

We introduce **MOMENT**, a family of open-source foundation models for general-purpose time series analysis. Pre-training large models on time series data is challenging due to (1) the absence of a large and cohesive public time series repository, and (2) diverse time series characteristics which make multi-dataset training onerous. Additionally, (3) experimental benchmarks to evaluate these models, especially in scenarios with limited resources, time, and supervision, are still in their nascent stages. To address these challenges, we compile a large and diverse collection of public time series, called the Time series Pile, and systematically tackle time series-specific challenges to unlock large-scale multi-dataset pre-training. Finally, we build on recent work to design a benchmark to evaluate time series foundation models on diverse tasks and datasets in limited supervision settings. Experiments on this benchmark demonstrate the effectiveness of our pre-trained models with minimal data and task-specific fine-tuning. Finally, we present several interesting empirical observations about large pre-trained time series models. Pre-trained models (`AutonLab/MOMENT-1-large`) and Time Series Pile (`AutonLab/Timeseries-PILE`) are available on https://huggingface.co/AutonLab.

1. Introduction

Time series analysis is an important field encompassing a wide range of applications ranging from forecasting weather patterns (Schneider & Dickinson, 1974) or detecting irregular heartbeats using Electrocardiograms (Goswami et al., 2021), to identifying anomalous software deployments (Xu et al., 2018). Due to its significant practical value and the
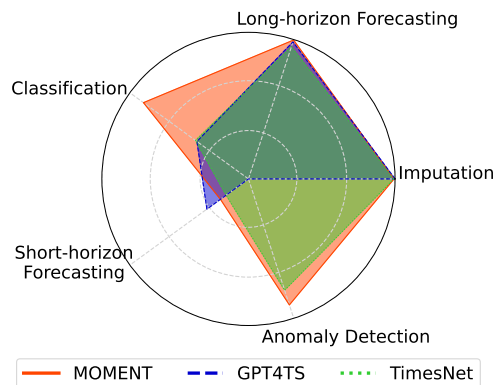

Figure 1. MOMENT can solve multiple time series analysis tasks well (App. F).

unique challenges that modeling time series data poses, time series analysis continues to receive substantial interest from academia and industry alike. However, modeling such data typically requires substantial domain expertise, time, and task-specific design.

Large pre-trained language (Touvron et al., 2023; Devlin et al., 2019; Chung et al., 2022), vision (Li et al., 2023a), and video (Day et al., 2023) models, typically perform well on a variety of tasks on data from diverse domains, with little or no supervision, and they can be specialized to perform well on specific tasks. We unlock these key capabilities for time series data and release the **first family of open-source large pre-trained time series models**, which we call MOMENT. The models in this family (1) serve as a building block for diverse **time series analysis tasks** (e.g., forecasting, classification, anomaly detection, and imputation, etc.), (2) are effective **out-of-the-box**, i.e., with no (or few) particular task-specific exemplars (enabling e.g., zero-shot forecasting, few-shot classification, etc.), and (3) are **tunable** using in-distribution and task-specific data to improve performance.

MOMENT is a family of high-capacity transformer models, pre-trained using a masked time series prediction task on large amounts of time series data drawn from diverse domains. Below we summarize our key contributions.

C1: Pre-training data. A key limiting factor for pre-training large time series models from scratch was the lack

*Equal contribution [1]Auton Lab, Robotics Institute, Carnegie Mellon University, Pittsburgh, USA [2]University of Pennsylvania, Philadelphia, USA. Correspondence to: Mononito Goswami <mgoswami@andrew.cmu.edu>.

of a large cohesive public time series data repositories (Zhou et al., 2023; Gruver et al., 2023; Jin et al., 2023; Ekambaram et al., 2024; Cao et al., 2023). Therefore, we compiled **The Time series Pile**, a large collection of publicly available data from diverse domains, ranging from healthcare to engineering to finance. The Time Series Pile comprises of over 5 public time series databases, from several diverse domains for pre-training and evaluation (Tab. 11).

C2: Multi-dataset pre-training. Unlike text and images, which have largely consistent sampling rates and number of channels, time series frequently vary in their temporal resolution, number of channels[1], lengths, and amplitudes, and sometimes have missing values. As a result, large-scale mixed dataset pre-training is largely unexplored. Instead, most methods are trained on a single dataset, and transferred across multiple datasets, but with modest success (Wu et al., 2023; Oreshkin et al., 2021; Narwariya et al., 2020).

C3: Evaluation. Holistic benchmarks to evaluate time series foundation models on diverse datasets and tasks are in their nascent stages. Recent studies (Goswami et al., 2023b) have highlighted the importance of well-defined benchmarks and large-scale experimentation in order to accurately assess the impact and effectiveness of novel methodologies. To evaluate MOMENT, we build on the multi-task time series modeling benchmark first proposed by Wu et al. (2023) along multiple dimensions. For each of the **5** time series modeling tasks, namely, short- and long-horizon forecasting, classification, anomaly detection, and imputation we evaluate MOMENT against (1) both state-of-the-art deep learning as well as statistical baselines, on (2) more task-specific datasets, (3) using multiple evaluation metrics, (4) exclusively in limited supervision settings (e.g., zero-shot imputation, linear probing for forecasting, unsupervised representation learning for classification).

Finally, we explore various properties of these pre-trained time series models. In particular, we study whether MOMENT is aware of intuitive time series characteristics such as frequency and trend, and the impact of initialization, model size scaling, and cross-modal transfer.

2. Related Work

Transformers and patching for time series modeling. There is a growing body of work utilizing transformers for various time series analysis tasks (Wen et al., 2023). One issue with applying transformers to time series data is the complexity of the self-attention mechanism, which grows quadratically with the size of input tokens (or length of time series) (Li et al., 2019). Nie et al. (2023) demonstrated that

treating time series sub-sequences (or patches) as tokens instead of individual time points is a simple, efficient, and effective mechanism for learning useful representations for forecasting. Drawing inspiration from prior work, we build on top of the transformer architecture which takes disjoint time series sub-sequences (or patches) as input.

Masked Representation Learning. Masked pre-training is a widely-used self-supervised learning task where a model learns to accurately reconstruct masked portions of its input. Masked language (Devlin et al., 2019; Raffel et al., 2020) and image modeling (Xie et al., 2022; Li et al., 2023b) have been successfully utilized to learn models from vast quantities of unlabeled data, which can generalize to a variety of downstream tasks.

For time series data, prior work has primarily focused on contrastive representation learning (Yue et al., 2022; Eldele et al., 2021; Franceschi et al., 2019). However, contrastive learning relies on data augmentation, which is both subjective and data-dependent. In contrast, some studies mask portions of time series using zeros and learn a model to reconstruct them (Nie et al., 2023; Zerveas et al., 2021; Dong et al., 2023; Li et al., 2023c).

Representation learning via masking is well-suited to all the downstream tasks we care about, especially forecasting and imputation, as they are instances of the masked reconstruction problem. Due to its simplicity and success in vision and language domains, we use the masked prediction task to pre-train our model, using a special embedding (see [MASK] in Fig. 3) to mask time series patches instead of zeros.

Cross-modal transfer learning using language models. Lu et al. (2022) had first shown that transformers pre-trained on text data (LLMs) can effectively solve sequence modeling tasks in other modalities. Subsequently, Shen et al. (2023) introduced ORCA, a general cross-modal fine-tuning framework that extends the applicability of a single large-scale pretrained model to diverse modalities by adapting to a target task via an align-then-refine workflow. Given the target input, ORCA first learns an embedding network that aligns the embedded feature distribution with the pre-training modality, then the pretrained model is fine-tuned on the embedded data, exploiting the knowledge shared across modalities. Some recent studies have leveraged this inherent ability of language pre-trained transformers to "reprogram" LLMs for time series analysis using parameter efficient fine-tuning and suitable tokenization strategies (Zhou et al., 2023; Gruver et al., 2023; Jin et al., 2023; Cao et al., 2023; Ekambaram et al., 2024). However, some of these models (Jin et al., 2023; Gruver et al., 2023) with billions of parameters demand significant memory and computational resources to perform well. We complement this line of research with three empirical observations (Sec 4.3): we show that (1) transformers trained on time series can also

---

[1]Temporal resolution reflects sampling frequency of time series (e.g., hourly, daily); Channel is a single univariate time series in multivariate data (Ekambaram et al., 2024).
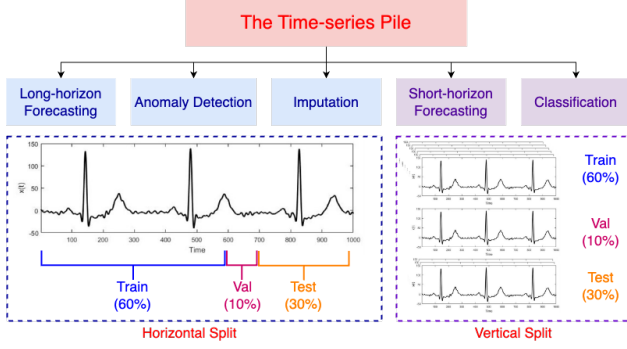
Figure 2. **Time Series Pile data splits**. To avoid data contamination, we carefully partition all datasets into disjoint train, validation, and test splits. We adhere to the predefined splits provided by the creators of each dataset. In cases where such splits are unavailable, we randomly sample 60% of the data for training, 10% for validation, and 30% for testing. We only use the training splits of all datasets for pre-training.

model sequences across modalities, (2) during pre-training, randomly initializing weights lead to lower pre-training loss, than initializing with language modeling weights, and (3) models pre-trained on time series outperform LLM-based models such as (Zhou et al., 2023; Jin et al., 2023) on many tasks and datasets.

Unanswered Questions. To the best of our knowledge, two questions remain largely unanswered in prior work on time series modeling. First, all existing time series models are (pre-)trained and fine-tuned on individual datasets (Nie et al., 2023; Yue et al., 2022; Wu et al., 2023; Zhou et al., 2023), and the benefits (or drawbacks) of large-scale multi-dataset pre-training remains unexplored (Wen et al., 2023). Second, there is very limited work on time series modeling in limited supervision settings, such as zero-shot forecasting (Oreshkin et al., 2021), or few-shot classification (Narwariya et al., 2020). In our work, we consider both these questions and *show that pre-training a model of sufficient capacity on a large corpus of unlabeled time series data can in fact enable it to provide reasonably accurate predictions in limited-supervision settings.*

3. Methodology

We first collect a large number of public time series data into the **Time Series Pile** and then use it to pre-train a **transformer model** on the **masked time series prediction task**. We discuss each of these steps in the following sections.

3.1. The Time Series Pile

Unlike natural language processing and computer vision, where large-scale datasets such as The Pile (Gao et al., 2020), and ImageNet-1K (Russakovsky et al., 2015) are

easily available for pre-training, public time series datasets are much smaller, scattered, and largely task-specific (Ma et al., 2023; Zhou et al., 2023; Gruver et al., 2023). To bridge this gap, we collate multiple time series from 4 task-specific, widely-used **public** repositories resulting in a large number of time series spanning diverse domains, and time series characteristics such as lengths, amplitudes, and temporal resolutions. We call this collection the Time Series Pile.

Informer long-horizon forecasting datasets (Zhou et al., 2021) is a collection of 9 datasets that are widely used to evaluate long-horizon forecasting performance (Wu et al., 2023; Nie et al., 2023; Challu et al., 2023): 2 hourly and minutely subsets of the Electricity Transformer Temperature (ETT) (Zhou et al., 2021), Electricity (Trindade, 2015), Traffic (California Department of Transportation, 2024), Weather (Max Planck Institute for Biogeochemistry, 2024), Influenza-like Illness (ILI) (Centers for Disease Control and Prevention, 2024), and Exchange-rate (Lai et al., 2018).

Monash time series forecasting archive (Godahewa et al., 2021) is a collection of 58 publicly available short-horizon forecasting datasets with a total of over 100K time series, spanning a variety of domains and temporal resolutions.

UCR/UEA classification archive (Dau et al., 2018) comprises of 159 time series datasets which are frequently used to benchmark classification algorithms (Ismail Fawaz et al., 2019). These datasets belonging to seven different categories (Image Outline, Sensor Readings, Motion Capture, Spectrographs, ECG, Electric Devices, and Simulated Data), vary substantially in terms of the number of classes and the size of the training set.

TSB-UAD anomaly benchmark (Paparrizos et al., 2022b) is a recent collection of 1980 univariate time series with labeled anomalies from 18 anomaly detection datasets proposed over the past decade. This collection includes both synthetic and real-world time series originating from a wide range of sources such as the human body, spaceships, environment, and web serves.

Minimizing data contamination using careful train-test splitting. We carefully split each dataset into disjoint training, validation, and test splits, based on splits specified by data creators. When these splits are not available, we randomly sample 60% of the data for training, 10% for validation, and 30% for testing. Long-horizon forecasting and anomaly detection datasets are typically long time series, which are split horizontally as shown in Fig. 2. Conversely, short-horizon forecasting and classification datasets often contain multiple short time series. For these datasets, a complete time series is either training, validation, or testing. We use the same random seed, set to 13, throughout our experiments, from pre-training to downstream evaluation,

thus ensuring that MOMENT only observes the training splits of datasets during pre-training.
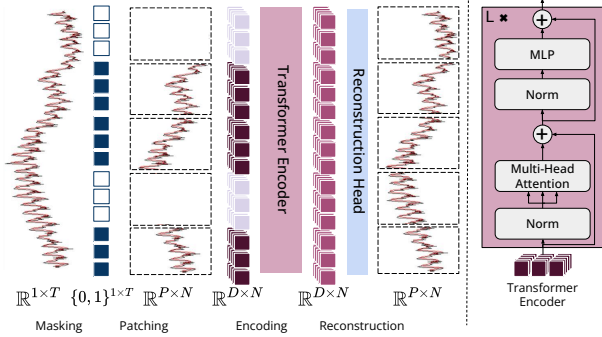
3.2. Model Architecture

$$\mathbb{R}^{1\times T} \quad \{0,1\}^{1\times T} \quad \mathbb{R}^{P\times N} \quad \mathbb{R}^{D\times N} \quad \mathbb{R}^{D\times N} \quad \mathbb{R}^{P\times N}$$

Masking   Patching   Encoding   Reconstruction   Transformer Encoder

Figure 3. **Overview of MOMENT**. A time series is broken into disjoint fixed-length sub-sequences called patches, and each patch is mapped into a D-dimensional patch embedding. During pre-training, we mask patches uniformly at random by replacing their patch embeddings using a special mask embedding [MASK]. The goal of pre-training is to learn patch embeddings which can be used to reconstruct the input time series using a light-weight reconstruction head.

MOMENT receives a univariate time series $\mathcal{T} \in \mathbb{R}^{1\times T}$, and a mask $M = \{0,1\}^{1\times T}$ of length T. 0 and 1 denote unobserved and observed time-stamps, respectively. Reversible instance normalization (Kim et al., 2022) is applied to the observed time series before breaking it into N disjoint patches of length P. Each patch is then mapped to a D-dimensional embedding, using a trainable linear projection if all time steps are observed, and a designated learnable mask embedding [MASK] $\in \mathbb{R}^{1\times D}$, otherwise. These N *patch embeddings* serve as input to the transformer model which retains their shape $(1 \times D)$ throughout its operations. Each transformed patch embedding is then used to reconstruct both masked and unmasked time series patches, using a *lightweight* prediction head. The goal of the prediction head is to map the transformed patch embeddings to the desired output dimensions. Since this particular prediction head enables time series reconstruction, we call it the *reconstruction head*. Fig. 3 shows an overview of our model.

Our transformer encoder retains the modifications proposed by Raffel et al. (2020) to the original Transformer (Vaswani et al., 2017). Specifically, we remove the additive bias from the Layer Norm (Ba et al., 2016), and place it before the residual skip connections (He et al., 2016), and use the relative positional embedding scheme (Shaw et al., 2018). Below we summarize the intuition behind some of our key design decisions.

Handling varying time series characteristics. Time series vary in length, number of channels, amplitudes, and tem-

poral resolutions. We address variable length by restricting MOMENT's input to a univariate time series of a fixed length $T = 512$. As is common practice, we sub-sample longer time series, and pad shorter ones with zeros on the left[2]. Moreover, segmenting time series into patches quadratically reduces MOMENT's memory footprint and computational complexity, and linearly increases the length of time series it can take as input. We handle multi-variate time series by independently operating on each channel along the batch dimension. Like recent studies (Zhou et al., 2023; Nie et al., 2023), we found that modeling each channel independently is an effective strategy for modeling multivariate time series. Finally, re-scaling and centering time series using reversible instance normalization enables MOMENT to model time series with significantly different temporal distributions (Kim et al., 2022). We did not explicitly model the temporal resolution of time series, since this information is often unavailable outside of time series forecasting datasets.

Intentionally simple encoder. Closely following the design of transformers in the language domain allows us to leverage their scalable and efficient implementations (e.g., gradient checkpointing, mixed precision training).

Light-weight prediction head. We use a lightweight prediction head instead of a decoder of the same size as the encoder, to enable the necessary architectural modifications for task-specific fine-tuning of a limited number of trainable parameters while keeping the bulk of parameters and the high-level features learned by the encoder intact.

Additional absolute positional embeddings. In addition to relative positional embeddings, we add absolute sinusoidal positional embeddings (Vaswani et al., 2017) to each patch[3].

3.3. Pre-training using Masked Time series Modeling

We pre-train MOMENT using the masked time series modeling task. Fig. 3 presents an overview of our pre-training procedure. During training, we first mask a small number of patches uniformly at random by replacing their patch embeddings with a learnable mask embedding [MASK]. The corrupted time series patches are then fed into the transformer encoder to learn patch representations, which are used to reconstruct the original time series using a lightweight reconstruction head. The pre-training objective is to minimize the *masked reconstruction error i.e.* the Mean Squared Error between the ground truth and the prediction, averaged over the masked patches.

---

[2]We found a large majority of classification datasets to have time series shorter than 512. Besides, a look-back window of length 512 was found to be sufficient for accurate long-horizon forecasting (Nie et al., 2023).

[3]We initially included absolute positional embeddings by accident, but subsequent experiments showed that combining absolute and relative positional embeddings improve predictions.

Tasks	Supervision	Datasets	Metrics	Baselines	Experimental Setting
Long-horizon Forecasting	Linear Probing	ETT-h1/h2/m1/m2, Electricity, Traffic, Weather, Exchange, ILI	MSE, MAE	Time-LLM, GPT4TS, TimesNet, PatchTST, FEDFormer, DLinear, N-BEATS, Stationary, LightTS	Look-back window $L = 512$, Forecast horizon $H = \{24, 60\}$ (ILI), $\{96, 720\}$ (rest)
Short-horizon Forecasting	Zero-shot	M3 and M4 competition datasets (subset)	sMAPE[4].	GPT4TS, TimesNet, N-BEATS, AutoARIMA, AutoTheta, AutoETS, Seasonal Naive, Naive, Random Walk	Statistical methods fit on individual time series. Deep learning methods are trained on a source dataset & evaluated on a target dataset of the same temporal resolution.
Classification	Unsupervised representation learning	UCR Classification Archive	Accuracy	GPT4TS, TimesNet, TS2Vec, T-Loss, TNC, TS-TCC, TST, CNN, Encoder, FCN, MCNN, MLP, ResNet, t-LeNet, TWIESN DTW	All models except MOMENT were trained on each individual dataset. Quality of unsupervised representations measured using the accuracy of a SVM trained on them.
Anomaly Detection	Linear probing, Zero-shot	UCR Anomaly Archive	Adjusted Best F1 VUS-ROC	GPT4TS, TimesNet, Anomaly Transformer, DGHL, Anomaly Nearest Neighbor	Reconstruction-based anomaly detection with window size $= 512$ MSE between observed and predicted time series is used as the anomaly criterion
Imputation	Linear probing, Zero-shot	ETT-h1/h2/m1/m2, Electricity, Weather	MSE, MAE	GPT4TS, TimesNet, Linear, Naive, Cubic Spline, Nearest Neighbors	Randomly mask contiguous sub-sequences of length 8 Masking ratios: $\{12.5\%, 25\%, 37.5\%, 50\%\}$

Table 1. **Experimental benchmark.** We evaluate MOMENT on 5 time series analysis tasks with an emphasis on limited memory, compute, and supervision settings.

Pre-training Setup. We pre-train three different sizes of MOMENT, roughly corresponding to the sizes of encoders in T5-Small, Base, and Large. Specifically, the Base (Small, Large) model uses a 12 (6, 24) layer Transform with hidden dimensions of size $D = 768$ (512, 1024), 12 (8, 16) attention heads, and feed-forward networks of size 3072 (2048, 4096), resulting in approximately 125 (40, 385) million parameters. All weights are randomly initialized before pre-training. All models take an input time series of length $T = 512$, breaking it into $N = 64$ disjoint patches of length $P = 8$. We mask 30% of the patches uniformly at random during pre-training.

We use the Adam optimizer with weight decay (Loshchilov & Hutter, 2019) with $\lambda = 0.05$, $\beta_1 = 0.9$, $\beta_2 = 0.999$. We clip the gradient at 5.0, train models using a batch size of 2048, and use cosine learning rate schedule with initial and final learning rates of $1e^{-4}$ and $1e^{-5}$, respectively. We use gradient checkpointing (Radford et al., 2021) to improve training throughput and save memory, and train all models in a mixed precision setting, using float-32 for numerically unstable operations, e.g. layer normalization, and bfloat-16[5], otherwise. We train all models for 2 epochs.

3.4. Fine-tuning on Downstream Tasks

MOMENT can be seamlessly used for multiple time series analysis tasks. In this work, we consider 5 practical time series analysis tasks as examples, namely: long- and short-horizon forecasting, classification, anomaly detection, and imputation. For forecasting tasks with horizon H, we replace the reconstruction head with a forecasting head, which first flattens all the N D-dimensional patch embeddings into a $N \times D$ dimensional vector, and then projects it into a H-dimensional time series via a linear projection layer. For all

other tasks, we retain the reconstruction head. We provide detailed descriptions of each task and MOMENT's configuration in App. F.

Fine-tuning settings. MOMENT can either be fine-tuned end-to-end, or linear probed (MOMENT$_{LP}$) by freezing all parameters except for those in the reconstruction or forecasting head. Additionally, for some tasks such as anomaly detection, unsupervised representation learning and imputation, MOMENT can also be used in a zero-shot (MOMENT$_0$) setting by retaining its reconstruction head.

4. Experimental Setup and Results

We extend the experimental benchmark introduced by Wu et al. (2023) across various dimensions. Below, we outline the design choices of our benchmark and highlight its key distinctions from TimesNet[6].

Time series modeling with limited supervision. Our benchmark comprises of 5 major time series modeling tasks of significant practical value, namely long- and short-horizon forecasting, imputation, classification, and anomaly detection, as outlined in Tab. 1. In contrast to TimesNet, we exclusively consider scenarios characterized by limited compute and supervision resources. These scenarios mimic practical situations where training (or fine-tuning) a deep neural network is infeasible due to resource limitations or insufficiently characterized data. Accordingly, we assess MOMENT in zero-shot settings whenever feasible and through linear probing for a few epochs otherwise.

For classification, we consider the unsupervised representation learning problem, where the goal is to learn representations of time series that are useful for downstream classification, without access to labeled data. As is common

---

[5]https://cloud.google.com/tpu/docs/bfloat16

[6]In this section, we use TimesNet to refer to the benchmark proposed by Wu et al. (2023) instead of their model.

Methods Metric	MOMENT$_{LP}$ MSE MAE	Time-LLM MSE MAE	GPT4TS MSE MAE	PatchTST MSE MAE	DLinear MSE MAE	TimesNet MSE MAE	FEDFormer MSE MAE	Stationary MSE MAE	LightTS MSE MAE	N-BEATS MSE MAE
Weather 96	0.154 0.209	- -	0.162 0.212	0.149 0.198	0.176 0.237	0.172 0.220	0.217 0.296	0.173 0.223	0.182 0.242	0.152 0.210
192	0.197 0.248	- -	0.204 0.248	0.194 0.241	0.220 0.282	0.219 0.261	0.276 0.336	0.245 0.285	0.227 0.287	0.199 0.260
336	0.246 0.285	- -	0.254 0.286	0.245 0.282	0.265 0.319	0.280 0.306	0.339 0.380	0.321 0.338	0.282 0.334	0.258 0.311
720	0.315 0.336	- -	0.326 0.337	0.314 0.334	0.333 0.362	0.365 0.359	0.403 0.428	0.414 0.410	0.352 0.386	0.331 0.359
ETTh1 96	0.387 0.410	0.408 0.429	0.376 0.397	0.370 0.399	0.375 0.399	0.384 0.402	0.376 0.419	0.513 0.491	0.424 0.432	0.399 0.428
192	0.410 0.426	- -	0.416 0.418	0.413 0.421	0.405 0.416	0.436 0.429	0.420 0.448	0.534 0.504	0.475 0.462	0.451 0.464
336	0.422 0.437	- -	0.442 0.433	0.422 0.436	0.439 0.443	0.491 0.469	0.459 0.465	0.588 0.535	0.518 0.488	0.498 0.500
720	0.454 0.472	0.523 0.514	0.477 0.456	0.447 0.466	0.472 0.490	0.521 0.500	0.506 0.507	0.643 0.616	0.547 0.533	0.608 0.573
ETTh2 96	0.288 0.345	0.285 0.348	0.285 0.342	0.274 0.336	0.289 0.353	0.340 0.374	0.358 0.397	0.476 0.458	0.397 0.437	0.327 0.387
192	0.349 0.386	- -	0.354 0.389	0.339 0.379	0.383 0.418	0.402 0.414	0.429 0.439	0.512 0.493	0.520 0.504	0.400 0.435
336	0.369 0.408	- -	0.373 0.407	0.329 0.380	0.448 0.465	0.452 0.452	0.496 0.487	0.552 0.551	0.626 0.559	0.747 0.599
720	0.403 0.439	0.399 0.435	0.406 0.441	0.379 0.422	0.605 0.551	0.462 0.468	0.463 0.474	0.562 0.560	0.863 0.672	1.454 0.847
ETTm1 96	0.293 0.349	0.384 0.403	0.292 0.346	0.290 0.342	0.299 0.343	0.338 0.375	0.379 0.419	0.386 0.398	0.374 0.400	0.318 0.367
192	0.326 0.368	- -	0.332 0.372	0.332 0.369	0.335 0.365	0.374 0.387	0.426 0.441	0.459 0.444	0.400 0.407	0.355 0.391
336	0.352 0.384	- -	0.366 0.394	0.366 0.392	0.369 0.386	0.410 0.411	0.445 0.459	0.495 0.464	0.438 0.438	0.401 0.419
720	0.405 0.416	0.437 0.429	0.417 0.421	0.416 0.420	0.425 0.421	0.478 0.450	0.543 0.490	0.585 0.516	0.527 0.502	0.448 0.448
ETTm2 96	0.170 0.260	0.181 0.269	0.173 0.262	0.165 0.255	0.167 0.269	0.187 0.267	0.203 0.287	0.192 0.274	0.209 0.308	0.197 0.271
192	0.227 0.297	- -	0.229 0.301	0.220 0.292	0.224 0.303	0.249 0.309	0.269 0.328	0.280 0.339	0.311 0.382	0.285 0.328
336	0.275 0.328	- -	0.286 0.341	0.274 0.329	0.281 0.342	0.321 0.351	0.325 0.366	0.334 0.361	0.442 0.466	0.338 0.366
720	0.363 0.387	0.366 0.388	0.378 0.401	0.362 0.385	0.397 0.421	0.408 0.403	0.421 0.415	0.417 0.413	0.675 0.587	0.395 0.419
ILI 24	2.728 1.114	3.025 1.195	2.063 0.881	1.319 0.754	2.215 1.081	2.317 0.934	3.228 1.260	2.294 0.945	8.313 2.144	4.539 1.528
36	2.669 1.092	- -	1.868 0.892	1.430 0.834	1.963 0.963	1.972 0.920	2.679 1.080	1.825 0.848	6.631 1.902	4.628 1.534
48	2.728 1.098	- -	1.790 0.884	1.553 0.815	2.130 1.024	2.238 0.940	2.622 1.078	2.010 0.900	7.299 1.982	4.957 1.585
60	2.883 1.126	3.245 1.221	1.979 0.957	1.470 0.788	2.368 1.096	2.027 0.928	2.857 1.157	2.178 0.963	7.283 1.985	5.429 1.661
ECL 96	0.136 0.233	- -	0.139 0.238	0.129 0.222	0.140 0.237	0.168 0.272	0.193 0.308	0.169 0.273	0.207 0.307	0.131 0.228
192	0.152 0.247	- -	0.153 0.251	0.157 0.240	0.153 0.249	0.184 0.289	0.201 0.315	0.182 0.286	0.213 0.316	0.153 0.248
336	0.167 0.264	- -	0.169 0.266	0.163 0.259	0.169 0.267	0.198 0.300	0.214 0.329	0.200 0.304	0.230 0.333	0.170 0.267
720	0.205 0.295	- -	0.206 0.297	0.197 0.290	0.203 0.301	0.220 0.320	0.246 0.355	0.222 0.321	0.265 0.360	0.208 0.298
Traffic 96	0.391 0.282	- -	0.388 0.282	0.360 0.249	0.410 0.282	0.593 0.321	0.587 0.366	0.612 0.338	0.615 0.391	0.375 0.259
192	0.404 0.287	- -	0.407 0.290	0.379 0.256	0.423 0.287	0.617 0.336	0.604 0.373	0.613 0.340	0.601 0.382	0.403 0.274
336	0.414 0.292	- -	0.412 0.294	0.392 0.264	0.436 0.296	0.629 0.336	0.621 0.383	0.618 0.328	0.613 0.386	0.426 0.285
720	0.450 0.310	- -	0.450 0.312	0.432 0.286	0.466 0.315	0.640 0.350	0.626 0.382	0.653 0.355	0.658 0.407	0.508 0.335

Table 2. Long-term forecasting performance measured using Mean Squared Error (MSE) and Mean Absolute Error (MAE). PatchTST performs the best across most settings, closely followed by MOMENT. Complete results in Tab. 18.

	Datasets	MOMENT$_{LP}$ M4	FR	GPT4TS M4	FR	TimesNet M4	FR	N-BEATS M4	FR	ARIMA	Theta	ETS	Seasonal Naive	Naive	Random Walk
M3	Yearly	**16.74**	**16.97**	18.39	**17.40**	27.48	**16.21**	**16.82**	**15.92**	17.90	16.70	16.47	17.54	17.54	16.77
	Quarterly	**10.09**	10.62	**10.18**	10.29	14.41	12.68	11.26	11.30	10.18	9.19	8.99	11.02	11.45	11.72
	Monthly	16.04	16.90	**15.21**	16.37	**15.58**	16.23	**15.63**	16.37	15.95	14.96	14.41	17.74	18.53	19.19
M4	Yearly	-	**14.84**	-	**14.80**	-	**14.40**	-	14.18	16.19	14.04	14.06	16.33	16.33	14.22
	Quarterly	-	12.02	-	11.77	-	13.21	-	12.25	10.86	10.21	10.24	12.55	11.65	11.46
	Monthly	-	15.80	-	15.36	-	15.67	-	15.24	13.68	13.19	13.58	16.00	15.24	15.48

Table 3. Zero-shot short-horizon forecasting performance on a subset of the M3 and M4 datasets measured using sMAPE. Statistical methods outperformed their deeper counterparts. However, on some datasets (in **bold**), MOMENT, GPT4TS and N-BEATS achieved a lower sMAPE than ARIMA.

in prior work (Yue et al., 2022; Franceschi et al., 2019), the quality of representations is measured using the accuracy of a Support Vector Machine trained on them (App. F.2). For short-horizon forecasting, we consider the zero-shot setting introduced by Oreshkin et al. (2021). In particular, we fine-tune MOMENT on a source dataset using a forecasting head, and evaluate its performance on a target dataset without any fine-tuning (App F.1.2, Tab. 21).

Datasets. We use the same datasets as TimesNet for forecasting and imputation. However, for classification and anomaly detection, we conduct experiments on larger and systematically chosen subset of datasets from the UCR classification archive (Dau et al., 2018) and UCR anomaly archive (Wu & Keogh, 2023). Specifically, we run classification experiments on all 91 time series datasets with each time series shorter than 512 time steps (Tab.23). For anomaly detection, while choosing the subset of time series, we prioritized coverage over different domains and data sources represented in the UCR anomaly archive (Tab. 22). We also note that the UCR anomaly archive was proposed as an improvement over pre-existing anomaly detection datasets such as the SMD (Su et al., 2019), and SMAP (Hundman et al., 2018), many of which are also used in TimesNet. Our proposed experimental setup is summarized in Tab. 1 and detailed in App. F.

Metrics. We evaluate each experiment using *multiple*

metrics used in task-specific benchmarks, such as MSE and MAE for long-horizon forecasting, and sMAPE for short-horizon forecasting. We also note that TimesNet and GPT4TS (Zhou et al., 2023) evaluate anomaly detection performance using vanilla F_1 score which ignores the sequential nature of time series. Instead, we measure anomaly detection performance with the widely used adjusted best F_1 score (Goswami et al., 2023a; Challu et al., 2022), and the recently proposed VUS-ROC (Paparrizos et al., 2022a).

Baselines. We compare MOMENT with state-of-the-art deep learning and statistical machine learning models across tasks (Tab. 35). This is in contrast to TimesNet which primarily compared with transformer-based approaches. These comparisons are crucial for assessing the practical utility of the proposed methods. We found that statistical and non-transformer-based approaches like ARIMA for short-horizon forecasting, N-BEATS for long-horizon forecasting, and k-nearest neighbors for anomaly detection outperform many deep and transformer-based models.

Hyper-parameter tuning. We do not perform hyper-parameter tuning. In all experiments that follow, unless mentioned otherwise, we fine-tune MOMENT-Large with a batch size of 64, and one cycle learning rate schedule with a peak learning rate between $5e-5$ and $1e-3$ (Smith & Topin, 2019). For baseline methods, we capture recommended settings from their papers and public repositories. We report all hyper-parameters settings for MOMENT and baselines in App. F.

Research questions. Through the following experiments we aim to answer 3 broad research questions.

RQ1: Effectiveness. Is MOMENT effective for multiple time series analysis tasks in limited supervision settings?

RQ2: Interpretability. What is MOMENT learning? Does it capture intuitive time series characteristics such as varying frequencies, trends, and amplitudes?

RQ3: Properties. What is the impact of the size of scaling model size? Can MOMENT, akin to LLMs, be used for cross-modal transfer learning?

4.1. MOMENT can solve multiple time series modeling tasks in limited supervision settings

Long-horizon forecasting. Linearly probing MOMENT achieves near state-of-the-art performance on most datasets and horizons, and is only second to PatchTST which generally achieves the lowest MSE (Tab. 2). On many datasets and horizons, forecasting models based on LLMs– TimeLLM and GPT4TS perform worse than MOMENT. Notably, N-BEATS outperforms several recent methods, emphasizing the importance of comparing forecasting performance beyond transformer-based approaches.

Zero-shot short-horizon forecasting. Among all tasks, we found zero-shot short-horizon forecasting to have the largest scope for improvement (Tab. 3). Statistical methods such as Theta and ETS outperformed their deeper counterparts. However, on some datasets, MOMENT achieved lower sMAPE than ARIMA.

Classification. Without any data-specific fine-tuning, MOMENT can learn distinct representations for different classes of data (Fig. 5), and an SVM trained on its representations performs better than all but 4 methods specifically built for time series classification models and trained on each individual dataset. Recently proposed GPT4TS and TimesNet perform poorly despite being trained on each individual dataset with labels.

Anomaly detection. On 44 time series from the UCR anomaly detection archive, MOMENT consistently outperformed both TimesNet and GPT4TS, as well as 2 state-of-the-art deep learning models tailored for anomaly detection, in both zero-shot and linear probing configurations. However, k-nearest neighbors performed marginally better in terms of VUS-ROC score, but had a lower adjusted best F_1 score.

Imputation. Tab. 6 contains imputation performance of all models averaged over 4 different masking rates. MOMENT with linear probing achieved the lowest reconstruction error on all ETT datasets. In the zero-shot setting, MOMENT consistently outperformed all statistical interpolation methods with the exception of linear interpolation.

4.2. What is MOMENT Learning?

We found that MOMENT can capture changes in intuitive time series characteristics such as trend, amplitude, frequencies, and phases of time series. However, it cannot differentiate between vertically shifted time series as it normalizes each signal prior to modeling (Fig. 4,7). Furthermore, on many classification datasets, MOMENT learns distinct representations of different classes, even in a zero-shot setting without access to labels (Fig. 5, 8).

4.3. Properties of Large Time Series Models

Model scaling improves training loss. Like LLMs, we found that increasing the size of the model leads to lower training loss, even before the first epoch (Fig. 6, left). An immediate next step is to assess how effectively this phenomenon extends to time series modeling tasks under limited supervision.

MOMENT can solve cross-modal sequence learning tasks. Lu et al. (2022) first showed that large pre-trained language and vision transformers can solve general sequence learning tasks for modalities outside of text and images with minimal fine-tuning. Several recent studies have leveraged these

	MOMENT$_0$	TimesNet	GPT4TS	TS2Vec	T-Loss	TNC	TS-TCC	TST	CNN	Encoder	FCN	MCNN	MLP	ResNet	t-LeNet	TWIESN	DTW
Mean	0.794	0.572	0.566	**0.851**	**0.833**	0.786	0.793	0.658	0.751	0.743	**0.809**	0.702	0.750	**0.825**	0.348	0.726	0.764
Median	0.815	0.565	0.583	**0.871**	**0.849**	0.788	0.802	0.720	0.773	0.753	**0.837**	0.718	0.766	**0.852**	0.333	0.724	0.768
Std.	0.147	0.238	0.234	0.134	0.136	0.168	0.176	0.220	0.180	0.159	0.188	0.194	0.169	0.177	0.221	0.164	0.152
Mean rank	7.2	13.3	13.3	3.5	5.3	6.9	6.5	11.8	9.4	8.9	5.6	11.0	9.2	4.4	16.1	10.4	9.1
Median rank	7.0	14.0	14.0	3.0	5.0	6.5	6.0	13.0	9.0	9.0	4.0	12.0	10.0	3.0	17.0	11.0	9.0
Wins	880	325	326	1220	1033	885	924	460	684	727	1031	533	696	1137	71	593	712
Losses	566	1121	1121	227	375	522	484	987	763	719	415	914	750	310	1375	854	734

Table 4. **Classification accuracy** of methods across 91 UCR datasets. Methods with mean and median accuracy higher than MOMENT are in **bold**. MOMENT without fine-tuning on individual datasets demonstrates promising accuracy. Complete results in Tab. 23. Results on multi-variate UEA datasets are in Tab. 24.

(i) Trend *(ii) Amplitude* *(iii) Frequency* *(iv) Baseline Shift* *(v) Phase*
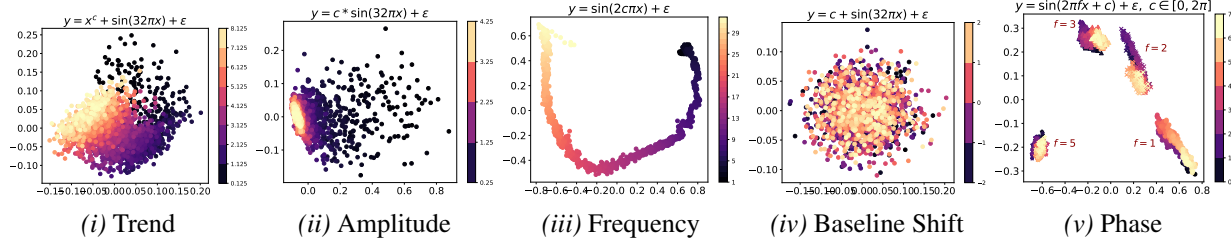
Figure 4. What is MOMENT learning? Principal components of the embeddings of synthetically generated sinusoids suggest that MOMENT can capture subtle trend, scale, frequency, and phase information. In each experiment, c controls the factor of interest, for example the power of the trend polynomial $c \in (\frac{1}{8}, 8)$ (Oreshkin et al., 2020) (Fig. 9), and frequency $c \in (1, 32)$ of the generated sine waves (Fig. 9). We generate multiple sine waves by varying c, derive their sequence-level representations using MOMENT, and visualize them in a 2-dimensional space using PCA and t-SNE (van der Maaten, 2014) in Fig. 4 and Fig. 7.

Model	Bit Memory	MNIST	CIFAR-10	IMDb
GPT-2	**1.000**	0.975	**0.711**	0.867
Flan-T5	**1.000**	**0.987**	0.672	0.861
MOMENT	**1.000**	0.982	0.620	**0.872**

Table 5. **Cross-modal transfer experiments.** Accuracy measured on the test set, from the checkpoint with the lowest train loss. Even with frozen self-attention and feed-forward layers, MOMENT is able to model cross-modal sequences on par with GPT-2 and Flan-T5 models of similar scale.

Figure 5. PCA and t-SNE visualizations of representations learned by MOMENT on the 3 largest UCR datasets. Different colors represent different classes. Even without dataset-specific fine-tuning, MOMENT learns distinct representations for different classes.
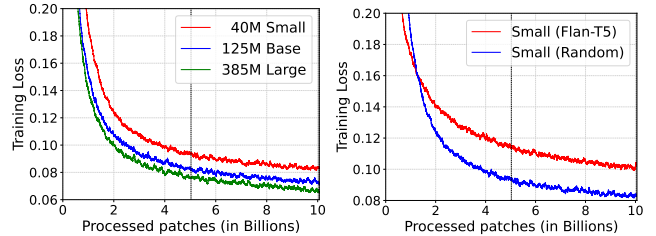
Figure 6. **Training losses (MSE).** A dashed vertical line denotes the first epoch. All models were trained with a batch size of 131072 patches. *(left)* Larger models obtain lower training loss. *right* Eventually, randomly initialized MOMENT-small outperforms the same model initialized with Flan-T5 weights.

properties to reprogram LLMs for time series tasks. We explore whether transformers pre-trained on time series can also be used to solve sequence classification tasks on image, text, and binary data. Our results confirm that by freezing the self-attention and feed-forward layers, MOMENT can model sequences comparable to GPT-2 and Flan-T5 models of similar scale (Tab. 5).

MOMENT with randomly initialized weights converges to a lower training loss. Our observations suggest that with sufficient data, pre-training our model from scratch results in a lower training loss than continually pre-training a model of similar size initialized with language modeling weights (Fig. 6, 12). This also underscores that there is sufficient publicly accessible pre-training data available in the Time Series Pile to facilitate pre-training time series foundation models from scratch.

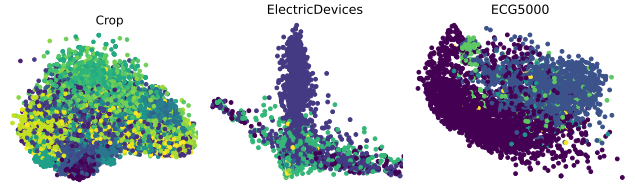| Dataset	MOMENT$_0$		MOMENT$_{LP}$		GPT4TS		TimesNet		Naive		Linear		Nearest		Cubic	
	MSE	MAE	MSE	MAE	MSE	MAE	MSE	MAE	MSE	MAE	MSE	MAE	MSE	MAE	MSE	MAE
Weather	0.082	0.130	0.035	0.075	**0.031**	**0.071**	0.036	0.098	0.119	0.108	0.065	0.067	0.083	0.078	0.601	0.153
ETTh1	0.402	0.403	**0.139**	**0.234**	0.227	0.254	0.175	0.264	1.185	0.658	0.775	0.534	0.900	0.579	2.178	0.916
ETTh2	0.125	0.238	**0.061**	**0.159**	0.109	0.213	0.170	0.286	0.225	0.304	0.135	0.234	0.166	0.252	1.920	0.641
ETTm1	0.202	0.288	**0.074**	**0.168**	0.076	0.146	0.087	0.198	0.455	0.365	0.165	0.229	0.230	0.260	0.858	0.494
ETTm2	0.078	0.184	**0.031**	**0.108**	0.052	0.133	0.112	0.220	0.113	0.191	0.062	0.138	0.079	0.152	0.534	0.356
Electricity	0.250	0.371	0.094	0.211	**0.072**	**0.183**	0.124	0.248	1.474	0.869	0.737	0.592	0.923	0.629	2.257	0.888

Table 6. **Imputation Results.** MOMENT with linear probing achieved the lowest reconstruction error on all ETT datasets. In the zero-shot setting, MOMENT consistently outperformed all statistical interpolation methods with the exception of linear interpolation. Complete results in Tab. 29.

Metric		MOMENT$_0$	MOMENT$_{LP}$	GPT4TS	TimesNet	Anomaly Transformer	DGHL	k-NN
Adj. F_1	Mean	0.585	**0.628**	0.424	0.537	0.492	0.425	0.554
	Median	0.683	**0.778**	0.331	0.541	0.432	0.331	0.595
	Std.	0.377	0.373	0.366	0.389	0.401	0.365	0.393
	Mean rank	3.410	**3.005**	4.862	3.642	4.326	5.071	3.681
	Median rank	**3.00**	**3.00**	5.00	3.50	4.00	5.25	3.75
	Wins/Losses	703/472	783/393	419/757	658/518	524/652	378/798	650/525
VUS ROC	Mean	0.670	0.684	0.611	0.679	0.661	0.646	**0.706**
	Median	0.677	0.692	0.615	0.692	0.658	0.635	**0.727**
	Std.	0.133	0.146	0.114	0.141	0.147	0.137	0.155
	Mean rank	4.056	3.382	5.193	3.897	3.913	4.403	**3.153**
	Median rank	4.00	**3.00**	6.00	4.00	4.00	4.50	3.00
	Wins/Losses	577/599	709/467	354/822	608/568	605/571	509/667	754/422

Table 7. Anomaly detection performance averaged over 248 time series from the UCR Anomaly Archive. MOMENT$_{LP}$ achieves near state-of-the-art anomaly detection results. Complete results in Tab. 22.

5. Conclusion and Future Work

We release the first open-source family of time series foundation models and make contributions at all stages of the development and evaluation process. We first compile a large and diverse collection of public time series, called the Time Series Pile, and demonstrate its efficacy by pre-training high-performing time series foundation models from scratch. Then, we systematically address several time series-specific challenges, which up to now have impeded widespread exploration of extensivelarge-scale multi-dataset pre-training.

We use the Time Series Pile and these strategies to pre-train transformer models of three different sizes. Finally, we design an experimental benchmark to evaluate time series foundation models on multiple practical time series tasks, particularly focusing on scenarios with constrained compute and supervision, building on prior work by Wu et al. (2023). Using this benchmark, we show that MOMENT is effective for the considered tasks with minimal fine-tuning. MOMENT's superior performance, especially on anomaly detection and classification problems which typically have small datasets, can be attributed to pre-training. Moreover, we demonstrate that across many tasks, smaller statistical and shallower deep learning methods perform reasonably well. Lastly, we make several interesting empirical observations about time series foundation models. Our overarching goal is to push the boundaries of open science by publicly releasing the Time Series Pile, along with code, model weights, and training logs.

We note several interesting directions of future work, including the application of MOMENT to real-world challenges, investigating multi-modal time series and text foundation models (Cai et al., 2023), and enhancing forecasting performance by pre-training MOMENT using causal attention and forecasting objectives.

Acknowledgments

Reproducibility statement

All models were trained and evaluated on a computing cluster consisting of 128 AMD EPYC 7502 CPUs, 503 GB of RAM, and 8 NVIDIA RTX A6000 GPUs each with 49 GiB RAM. All MOMENT variants were trained on a single A6000 GPU (with any data or model parallelism). We have made MOMENT-large[7] and the Time Series Pile[8] publicly available on Huggingface. We are working on open-sourcing MOMENT-base and MOMENT-small, and our research code public. The latter is currently available at https://github.com/moment-timeseries-foundation-model/moment-research. We enlist an exhaustive list of hyper-parameters in App. F to aid reproducibility. We would like to emphasize that all datasets used in this study are publicly available.

---

[7]https://huggingface.co/AutonLab/MOMENT-1-large

[8]https://huggingface.co/datasets/AutonLab/Timeseries-PILE

Impact statement

Transparency Index. Given the exponential rise in societal reliance on large foundation models, ensuring transparency in their training approach, architecture, and downstream application is crucial for public accountability, scientific advancement, and effective governance. o uphold this objective, we publicly release our training code base, data sources, and evaluation pipeline. We assess the transparency of MOMENT using the criteria outlined by Bommasani et al. (2023), focusing on upstream resources utilized during training and model description, encompassing 32 and 33 transparency indicators, respectively. We report expected upstream and model transparency scores for MOMENT in Tab. 34. Notably, MOMENT is *expected* to have one of the highest levels of upstream transparency. However, it's model transparency scores are lower, primarily due to comprehensive (external and third-party) harm and trustworthiness evaluations, which are not well understood in the context of time series modeling.

Environmental Impact. We train multiple models over many days resulting in significant energy usage and a sizeable carbon footprint. However, we hope that releasing our models will ensure that future time series modeling efforts are quicker and more efficient, resulting in lower carbon emissions.

We follow prior work (Bender et al., 2021; Patterson et al., 2021; Touvron et al., 2023; Wu et al., 2022; Dodge et al., 2022) and estimate the carbon footprint of pre-training all variants of MOMENT based on the GPU device used and the carbon efficiency of the electricity grid. Our estimated CO_2 generation estimates are shown in Tab. 8.

We use the Total Graphics Power (TGP) to calculate the total power consumed for training MOMENT models, although the total power consumed by the GPU will likely vary a little based on the GPU utilization while training our model. Our calculations do not account for power demands from other sources of our compute. We use 336.566 Kg $C0_2$/MWH as the standard value of CO_2 emission per megawatt hour of energy consumed for Pittsburgh[9].

We share an upper limit of the individual CO_2 emission for each model, as well as a more realistic actual estimate for the carbon emissions from MOMENT-small and MOMENT-base, since they were trained simultaneously on a single Nvidia RTX A6000 GPU, and thus the power consumed by the GPU was shared for the training of both variants. MOMENT-large was trained independently on a single RTX A6000 GPU.

Ethical considerations and potential misuse. Despite MOMENT's promising performance in limited-data settings,

---

[9]https://emissionsindex.org/

Model Variant	# Parameters (M)	GPU Hours	Power Consumption (W)	Carbon Emission (tCO2eq)
Small	40	308.378	300	31.136
Base	125	308.306	300	31.129
Large	385	404.389	300	40.831
Upper Bound Total	-	1021.073	300	103.096
Actual Total	-	712.767	300	71.967

Table 8. Total carbon emission induced upon training the `MOMENT` family of models. `MOMENT-small` and `MOMENT-base` were trained simultaneously on a single GPU, thus the TGP required for each model would likely be much less than 300W, and the total time for both models combined is equal to the maximum of the time required for each model. Actual total power consumption and carbon emission values account for this.

it's important to use its predictions with care, especially in high-stakes settings like healthcare. The reliability of `MOMENT`'s predictions hinges on the quality and diversity of the data it was trained on. Any dependence on unreliable or biased data could potentially result in skewed outputs, unfairly portraying or discriminating against certain groups or individuals. While `MOMENT` demonstrates the ability to capture changes time-series characteristics, e.g. trend, amplitude, frequency, it struggles to differentiate between vertically shifted time-series as it normalizes signals prior to modeling. Greater interpretability and explainability of `MOMENT`'s predictions are necessary to enable more informed decision-making processes. Prior to utilizing `MOMENT` in high-stakes decision-making, we recommend fine-tuning and evaluating the model with task-specific, in-domain data to address these ethical concerns and ensure equitable outcomes. Additionally, efforts should be made to promote equitable access to `MOMENT` and other AI technologies, particularly within healthcare systems where disparities in access may exacerbate existing inequities.

References

Ansari, A. F., Stella, L., Turkmen, C., Zhang, X., Mercado, P., Shen, H., Shchur, O., Rangapuram, S. S., Arango, S. P., Kapoor, S., et al. Chronos: Learning the language of time series. *arXiv preprint arXiv:2403.07815*, 2024.

Ba, J. L., Kiros, J. R., and Hinton, G. E. Layer normalization, 2016.

Bao, H., Dong, L., Piao, S., and Wei, F. BEit: BERT pre-training of image transformers. In *International Conference on Learning Representations*, 2022. URL https://openreview.net/forum?id=p-BhZSz59o4.

Bender, E. M., Gebru, T., McMillan-Major, A., and Shmitchell, S. On the dangers of stochastic parrots: Can language models be too big? In *Proceedings of the 2021 ACM Conference on Fairness, Accountability, and Transparency*, FAccT '21, pp. 610–623, New York, NY, USA, 2021. Association for Computing Machinery. ISBN 9781450383097. doi: 10.1145/

3442188.3445922. URL https://doi.org/10.1145/3442188.3445922.

Bommasani, R., Klyman, K., Longpre, S., Kapoor, S., Maslej, N., Xiong, B., Zhang, D., and Liang, P. The foundation model transparency index, 2023.

Cai, Y., Goswami, M., Choudhry, A., Srinivasan, A., and Dubrawski, A. Jolt: Jointly learned representations of language and time-series. In *Deep Generative Models for Health Workshop NeurIPS 2023*, 2023.

California Department of Transportation. Performance measurement system (pems), 2024. URL http://pems.dot.ca.gov/. Accessed: 2024-02-01.

Cao, D., Jia, F., Arik, S. O., Pfister, T., Zheng, Y., Ye, W., and Liu, Y. Tempo: Prompt-based generative pre-trained transformer for time series forecasting, 2023.

Centers for Disease Control and Prevention. Fluview: Flu activity & surveillance, 2024. URL https://gis.cdc.gov/grasp/fluview/fluportaldashboard.html. Accessed: 2024-02-01.

Challu, C., Olivares, K. G., Oreshkin, B. N., Garza Ramirez, F., Mergenthaler Canseco, M., and Dubrawski, A. NHITS: Neural hierarchical interpolation for time series forecasting. *Proceedings of the AAAI Conference on Artificial Intelligence*, 37(6):6989–6997, Jun. 2023. doi: 10.1609/aaai.v37i6.25854. URL https://ojs.aaai.org/index.php/AAAI/article/view/25854.

Challu, C. I., Jiang, P., Nian Wu, Y., and Callot, L. Deep generative model with hierarchical latent factors for time series anomaly detection. In Camps-Valls, G., Ruiz, F. J. R., and Valera, I. (eds.), *Proceedings of The 25th International Conference on Artificial Intelligence and Statistics*, volume 151 of *Proceedings of Machine Learning Research*, pp. 1643–1654. PMLR, 28–30 Mar 2022. URL https://proceedings.mlr.press/v151/challu22a.html.

Chung, H. W., Hou, L., Longpre, S., Zoph, B., Tay, Y., Fedus, W., Li, Y., Wang, X., Dehghani, M., Brahma, S., et al. Scaling instruction-finetuned language models. *arXiv preprint arXiv:2210.11416*, 2022.

Cui, Z., Chen, W., and Chen, Y. Multi-scale convolutional neural networks for time series classification, 2016.

Das, A., Kong, W., Sen, R., and Zhou, Y. A decoder-only foundation model for time-series forecasting. *arXiv preprint arXiv:2310.10688*, 2023.

Dau, H. A., Keogh, E., Kamgar, K., Yeh, C.-C. M., Zhu, Y., Gharghabi, S., Ratanamahatana, C. A., Yanping, Hu, B., Begum, N., Bagnall, A., Mueen, A., Batista, G., and Hexagon-ML. The ucr time series classification archive, October 2018. https://www.cs.ucr.edu/~eamonn/time_series_data_2018/.

Day, K., Christl, D., Salvi, R., and Sriram, P. Video pre-trained transformer: A multimodal mixture of pre-trained experts, 2023.

Devlin, J., Chang, M.-W., Lee, K., and Toutanova, K. BERT: Pre-training of deep bidirectional transformers for language understanding. In Burstein, J., Doran, C., and Solorio, T. (eds.), *Proceedings of the 2019 Conference of the North American Chapter of the Association for Computational Linguistics: Human Language Technologies, Volume 1 (Long and Short Papers)*, pp. 4171–4186, Minneapolis, Minnesota, June 2019. Association for Computational Linguistics. doi: 10.18653/v1/N19-1423. URL https://aclanthology.org/N19-1423.

Dodge, J., Prewitt, T., Tachet des Combes, R., Odmark, E., Schwartz, R., Strubell, E., Luccioni, A. S., Smith, N. A., DeCario, N., and Buchanan, W. Measuring the carbon intensity of ai in cloud instances. In *Proceedings of the 2022 ACM Conference on Fairness, Accountability, and Transparency*, FAccT '22, pp. 1877–1894, New York, NY, USA, 2022. Association for Computing Machinery. ISBN 9781450393522. doi: 10.1145/3531146.3533234. URL https://doi.org/10.1145/3531146.3533234.

Dong, J., Wu, H., Zhang, H., Zhang, L., Wang, J., and Long, M. Simmtm: A simple pre-training framework for masked time-series modeling. In *Advances in Neural Information Processing Systems*, 2023.

Dosovitskiy, A., Beyer, L., Kolesnikov, A., Weissenborn, D., Zhai, X., Unterthiner, T., Dehghani, M., Minderer, M., Heigold, G., Gelly, S., Uszkoreit, J., and Houlsby, N. An image is worth 16x16 words: Transformers for image recognition at scale. In *International Conference on Learning Representations*, 2021. URL https://openreview.net/forum?id=YicbFdNTTy.

Ekambaram, V., Jati, A., Nguyen, N. H., Dayama, P., Reddy, C., Gifford, W. M., and Kalagnanam, J. Tiny time mixers (ttms): Fast pre-trained models for enhanced zero/few-shot forecasting of multivariate time series, 2024.

Eldele, E., Ragab, M., Chen, Z., Wu, M., Kwoh, C. K., Li, X., and Guan, C. Time-series representation learning via temporal and contextual contrasting. In Zhou, Z.-H. (ed.), *Proceedings of the Thirtieth International Joint Conference on Artificial Intelligence, IJCAI-21*, pp. 2352–2359. International Joint Conferences on Artificial Intelligence Organization, 8 2021. doi: 10.24963/ijcai.2021/324. URL https://doi.org/10.24963/ijcai.2021/324. Main Track.

Franceschi, J.-Y., Dieuleveut, A., and Jaggi, M. Unsupervised scalable representation learning for multivariate time series. In Wallach, H., Larochelle, H., Beygelzimer, A., d'Alché-Buc, F., Fox, E., and Garnett, R. (eds.), *Advances in Neural Information Processing Systems*, volume 32. Curran Associates, Inc., 2019. URL https://proceedings.neurips.cc/paper_files/paper/2019/file/53c6de78244e9f528eb3e1cda69699bb-Paper.pdf.

Gao, L., Biderman, S., Black, S., Golding, L., Hoppe, T., Foster, C., Phang, J., He, H., Thite, A., Nabeshima, N., Presser, S., and Leahy, C. The pile: An 800gb dataset of diverse text for language modeling, 2020.

Garza, A. and Mergenthaler-Canseco, M. Timegpt-1. *arXiv preprint arXiv:2310.03589*, 2023.

Garza, F., Mergenthaler Canseco, M., Challú, C., and Olivares, K. StatsForecast: Lightning fast forecasting with statistical and econometric models. PyCon Salt Lake City, Utah, US 2022, 2022. URL https://github.com/Nixtla/statsforecast.

Godahewa, R. W., Bergmeir, C., Webb, G. I., Hyndman, R., and Montero-Manso, P. Monash time series forecasting archive. In *Thirty-fifth Conference on Neural Information Processing Systems Datasets and Benchmarks Track (Round 2)*, 2021. URL https://openreview.net/forum?id=wEc1mgAjU-.

Goswami, M., Boecking, B., and Dubrawski, A. Weak supervision for affordable modeling of electrocardiogram data. In *AMIA Annual Symposium Proceedings*, volume 2021, pp. 536. American Medical Informatics Association, 2021.

Goswami, M., Challu, C. I., Callot, L., Minorics, L., and Kan, A. Unsupervised model selection for time series anomaly detection. In *The Eleventh International Conference on Learning Representations*, 2023a. URL https://openreview.net/forum?id=gOZ_pKANaPW.

Goswami, M., Sanil, V., Choudhry, A., Srinivasan, A., Udompanyawit, C., and Dubrawski, A. AQua: A benchmarking tool for label quality assessment. In *Thirty-seventh Conference on Neural Information Processing Systems Datasets and Benchmarks Track*, 2023b. URL https://openreview.net/forum?id=dhJ8VbcEtX.

Gruver, N., Finzi, M. A., Qiu, S., and Wilson, A. G. Large language models are zero-shot time series forecasters. In *Thirty-seventh Conference on Neural Information Processing Systems*, 2023. URL https://openreview.net/forum?id=md68e8iZK1.

He, K., Zhang, X., Ren, S., and Sun, J. Deep residual learning for image recognition. In *2016 IEEE Conference on Computer Vision and Pattern Recognition (CVPR)*, pp. 770–778, 2016. doi: 10.1109/CVPR.2016.90.

Hundman, K., Constantinou, V., Laporte, C., Colwell, I., and Soderstrom, T. Detecting spacecraft anomalies using lstms and nonparametric dynamic thresholding. In *Proceedings of the 24th ACM SIGKDD international conference on knowledge discovery & data mining*, pp. 387–395, 2018.

Ismail Fawaz, H., Forestier, G., Weber, J., Idoumghar, L., and Muller, P.-A. Deep learning for time series classification: a review. *Data Mining and Knowledge Discovery*, 33(4):917–963, 2019.

Jin, M., Wang, S., Ma, L., Chu, Z., Zhang, J. Y., Shi, X., Chen, P.-Y., Liang, Y., Li, Y.-F., Pan, S., and Wen, Q. Time-llm: Time series forecasting by reprogramming large language models, 2023.

Kim, T., Kim, J., Tae, Y., Park, C., Choi, J.-H., and Choo, J. Reversible instance normalization for accurate time-series forecasting against distribution shift. In *International Conference on Learning Representations*, 2022. URL https://openreview.net/forum?id=cGDAkQo1C0p.

Lai, G., Chang, W.-C., Yang, Y., and Liu, H. Modeling long- and short-term temporal patterns with deep neural networks. In *The 41st International ACM SIGIR Conference on Research & Development in Information Retrieval*, SIGIR '18, pp. 95–104, New York, NY, USA, 2018. Association for Computing Machinery. ISBN 9781450356572. doi: 10.1145/3209978.3210006. URL https://doi.org/10.1145/3209978.3210006.

Le Guennec, A., Malinowski, S., and Tavenard, R. Data Augmentation for Time Series Classification using Convolutional Neural Networks. In *ECML/PKDD Workshop on Advanced Analytics and Learning on Temporal Data*, Riva Del Garda, Italy, September 2016. URL https://shs.hal.science/halshs-01357973.

Li, J., Li, D., Savarese, S., and Hoi, S. Blip-2: Bootstrapping language-image pre-training with frozen image encoders and large language models. *arXiv preprint arXiv:2301.12597*, 2023a.

Li, S., Jin, X., Xuan, Y., Zhou, X., Chen, W., Wang, Y.-X., and Yan, X. Enhancing the locality and breaking the memory bottleneck of transformer on time series forecasting. *Advances in neural information processing systems*, 32, 2019.

Li, Y., Fan, H., Hu, R., Feichtenhofer, C., and He, K. Scaling language-image pre-training via masking. In *2023 IEEE/CVF Conference on Computer Vision and Pattern Recognition (CVPR)*, pp. 23390–23400, Los Alamitos, CA, USA, jun 2023b. IEEE Computer Society. doi: 10.1109/CVPR52729.2023.02240. URL https://doi.ieeecomputersociety.org/10.1109/CVPR52729.2023.02240.

Li, Z., Rao, Z., Pan, L., Wang, P., and Xu, Z. Ti-mae: Self-supervised masked time series autoencoders, 2023c.

Liu, S., Yu, H., Liao, C., Li, J., Lin, W., Liu, A. X., and Dustdar, S. Pyraformer: Low-complexity pyramidal attention for long-range time series modeling and forecasting. In *International Conference on Learning Representations*, 2022. URL https://openreview.net/forum?id=0EXmFzUn5I.

Liu, Y., Hu, T., Zhang, H., Wu, H., Wang, S., Ma, L., and Long, M. itransformer: Inverted transformers are effective for time series forecasting. *arXiv preprint arXiv:2310.06625*, 2023.

Liu, Y., Zhang, H., Li, C., Huang, X., Wang, J., and Long, M. Timer: Generative pre-trained transformers are large time series models. In *Forty-first International Conference on Machine Learning*, 2024.

Loshchilov, I. and Hutter, F. Decoupled weight decay regularization. In *International Conference on Learning Representations*, 2019. URL https://openreview.net/forum?id=Bkg6RiCqY7.

Lu, K., Grover, A., Abbeel, P., and Mordatch, I. Frozen pretrained transformers as universal computation engines. *Proceedings of the AAAI Conference on Artificial Intelligence*, 36(7):7628–7636, Jun. 2022. doi: 10.1609/aaai.v36i7.20729. URL https://ojs.aaai.org/index.php/AAAI/article/view/20729.

Ma, Q., Liu, Z., Zheng, Z., Huang, Z., Zhu, S., Yu, Z., and Kwok, J. T. A survey on time-series pre-trained models, 2023.

Max Planck Institute for Biogeochemistry. Weather data, 2024. URL https://www.bgc-jena.mpg.de/wetter/. Accessed: 2024-02-01.

Narwariya, J., Malhotra, P., Vig, L., Shroff, G., and Vishnu, T. V. Meta-learning for few-shot time series classification. In *Proceedings of the 7th ACM IKDD CoDS and 25th COMAD*, CoDS COMAD 2020, pp. 28–36, New York, NY, USA, 2020. Association for Computing Machinery. ISBN 9781450377386. doi: 10.1145/3371158.3371162. URL https://doi.org/10.1145/3371158.3371162.

Nie, Y., Nguyen, N. H., Sinthong, P., and Kalagnanam, J. A time series is worth 64 words: Long-term forecasting with transformers. In *The Eleventh International Conference on Learning Representations*, 2023. URL https://openreview.net/forum?id=Jbdc0vTOcol.

Oreshkin, B. N., Carpov, D., Chapados, N., and Bengio, Y. N-beats: Neural basis expansion analysis for interpretable time series forecasting. In *International Conference on Learning Representations*, 2020. URL https://openreview.net/forum?id=r1ecqn4YwB.

Oreshkin, B. N., Carpov, D., Chapados, N., and Bengio, Y. Meta-learning framework with applications to zero-shot time-series forecasting. *Proceedings of the AAAI Conference on Artificial Intelligence*, 35(10): 9242–9250, May 2021. doi: 10.1609/aaai.v35i10.17115. URL https://ojs.aaai.org/index.php/AAAI/article/view/17115.

Paparrizos, J., Boniol, P., Palpanas, T., Tsay, R. S., Elmore, A., and Franklin, M. J. Volume under the surface: A new accuracy evaluation measure for time-series anomaly detection. *Proc. VLDB Endow.*, 15(11): 2774–2787, jul 2022a. ISSN 2150-8097. doi: 10.14778/3551793.3551830. URL https://doi.org/10.14778/3551793.3551830.

Paparrizos, J., Kang, Y., Boniol, P., Tsay, R. S., Palpanas, T., and Franklin, M. J. Tsb-uad: An end-to-end benchmark suite for univariate time-series anomaly detection. *Proc. VLDB Endow.*, 15(8):1697–1711, apr 2022b. ISSN 2150-8097. doi: 10.14778/3529337.3529354. URL https://doi.org/10.14778/3529337.3529354.

Patterson, D., Gonzalez, J., Le, Q., Liang, C., Munguia, L.-M., Rothchild, D., So, D., Texier, M., and Dean, J. Carbon emissions and large neural network training, 2021.

Radford, A., Kim, J. W., Hallacy, C., Ramesh, A., Goh, G., Agarwal, S., Sastry, G., Askell, A., Mishkin, P., Clark, J., Krueger, G., and Sutskever, I. Learning transferable visual models from natural language supervision. In Meila, M. and Zhang, T. (eds.), *Proceedings of the 38th International Conference on Machine Learning*, volume 139 of *Proceedings of Machine Learning Research*, pp. 8748–8763. PMLR, 18–24 Jul

2021. URL https://proceedings.mlr.press/v139/radford21a.html.

Raffel, C., Shazeer, N., Roberts, A., Lee, K., Narang, S., Matena, M., Zhou, Y., Li, W., and Liu, P. J. Exploring the limits of transfer learning with a unified text-to-text transformer. *Journal of Machine Learning Research*, 21(140):1–67, 2020. URL http://jmlr.org/papers/v21/20-074.html.

Ramaswamy, S., Rastogi, R., and Shim, K. Efficient algorithms for mining outliers from large data sets. In *Proceedings of the 2000 ACM SIGMOD International Conference on Management of Data*, SIGMOD '00, pp. 427–438, New York, NY, USA, 2000. Association for Computing Machinery. ISBN 1581132174. doi: 10.1145/342009.335437. URL https://doi.org/10.1145/342009.335437.

Rasul, K., Ashok, A., Williams, A. R., Khorasani, A., Adamopoulos, G., Bhagwatkar, R., Biloš, M., Ghonia, H., Hassen, N. V., Schneider, A., et al. Lag-llama: Towards foundation models for time series forecasting. *arXiv preprint arXiv:2310.08278*, 2023.

Russakovsky, O., Deng, J., Su, H., Krause, J., Satheesh, S., Ma, S., Huang, Z., Karpathy, A., Khosla, A., Bernstein, M., Berg, A. C., and Fei-Fei, L. ImageNet Large Scale Visual Recognition Challenge. *International Journal of Computer Vision (IJCV)*, 115(3):211–252, 2015. doi: 10.1007/s11263-015-0816-y.

Schmidl, S., Wenig, P., and Papenbrock, T. Anomaly detection in time series: A comprehensive evaluation. *Proc. VLDB Endow.*, 15(9):1779–1797, may 2022. ISSN 2150-8097. doi: 10.14778/3538598.3538602. URL https://doi.org/10.14778/3538598.3538602.

Schneider, S. H. and Dickinson, R. E. Climate modeling. *Reviews of Geophysics*, 12(3):447–493, 1974.

Serrà, J., Pascual, S., and Karatzoglou, A. Towards a universal neural network encoder for time series. In *International Conference of the Catalan Association for Artificial Intelligence*, 2018. URL https://api.semanticscholar.org/CorpusID:13675490.

Shaw, P., Uszkoreit, J., and Vaswani, A. Self-attention with relative position representations. *arXiv preprint arXiv:1803.02155*, 2018.

Shen, J., Li, L., Dery, L. M., Staten, C., Khodak, M., Neubig, G., and Talwalkar, A. Cross-modal fine-tuning: Align then refine, 2023.

Smith, L. N. and Topin, N. Super-convergence: Very fast training of neural networks using large learning rates.

In *Artificial intelligence and machine learning for multi-domain operations applications*, volume 11006, pp. 369–386. SPIE, 2019.

Su, Y., Zhao, Y., Niu, C., Liu, R., Sun, W., and Pei, D. Robust anomaly detection for multivariate time series through stochastic recurrent neural network. In *Proceedings of the 25th ACM SIGKDD international conference on knowledge discovery & data mining*, pp. 2828–2837, 2019.

Talukder, S., Yue, Y., and Gkioxari, G. Totem: Tokenized time series embeddings for general time series analysis, 2024.

Tanisaro, P. and Heidemann, G. Time series classification using time warping invariant echo state networks. In *2016 15th IEEE International Conference on Machine Learning and Applications (ICMLA)*, pp. 831–836, 2016. doi: 10.1109/ICMLA.2016.0149.

Tolstikhin, I. O., Houlsby, N., Kolesnikov, A., Beyer, L., Zhai, X., Unterthiner, T., Yung, J., Steiner, A., Keysers, D., Uszkoreit, J., et al. Mlp-mixer: An all-mlp architecture for vision. *Advances in neural information processing systems*, 34:24261–24272, 2021.

Tonekaboni, S., Eytan, D., and Goldenberg, A. Unsupervised representation learning for time series with temporal neighborhood coding. In *International Conference on Learning Representations*, 2021. URL https://openreview.net/forum?id=8qDwejCuCN.

Touvron, H., Martin, L., Stone, K., Albert, P., Almahairi, A., Babaei, Y., Bashlykov, N., Batra, S., Bhargava, P., Bhosale, S., Bikel, D., Blecher, L., Ferrer, C. C., Chen, M., Cucurull, G., Esiobu, D., Fernandes, J., Fu, J., Fu, W., Fuller, B., Gao, C., Goswami, V., Goyal, N., Hartshorn, A., Hosseini, S., Hou, R., Inan, H., Kardas, M., Kerkez, V., Khabsa, M., Kloumann, I., Korenev, A., Koura, P. S., Lachaux, M.-A., Lavril, T., Lee, J., Liskovich, D., Lu, Y., Mao, Y., Martinet, X., Mihaylov, T., Mishra, P., Molybog, I., Nie, Y., Poulton, A., Reizenstein, J., Rungta, R., Saladi, K., Schelten, A., Silva, R., Smith, E. M., Subramanian, R., Tan, X. E., Tang, B., Taylor, R., Williams, A., Kuan, J. X., Xu, P., Yan, Z., Zarov, I., Zhang, Y., Fan, A., Kambadur, M., Narang, S., Rodriguez, A., Stojnic, R., Edunov, S., and Scialom, T. Llama 2: Open foundation and fine-tuned chat models, 2023.

Trindade, A. ElectricityLoadDiagrams20112014. UCI Machine Learning Repository, 2015. DOI: https://doi.org/10.24432/C58C86.

Van Den Oord, A., Vinyals, O., et al. Neural discrete representation learning. *Advances in neural information processing systems*, 30, 2017.

van der Maaten, L. Accelerating t-sne using tree-based algorithms. *Journal of Machine Learning Research*, 15 (93):3221–3245, 2014. URL http://jmlr.org/papers/v15/vandermaaten14a.html.

Vaswani, A., Shazeer, N., Parmar, N., Uszkoreit, J., Jones, L., Gomez, A. N., Kaiser, L. u., and Polosukhin, I. Attention is all you need. In Guyon, I., Luxburg, U. V., Bengio, S., Wallach, H., Fergus, R., Vishwanathan, S., and Garnett, R. (eds.), *Advances in Neural Information Processing Systems*, volume 30. Curran Associates, Inc., 2017. URL https://proceedings.neurips.cc/paper_files/paper/2017/file/3f5ee243547dee91fbd053c1c4a845aa-Paper.pdf.

Wang, Z., Yan, W., and Oates, T. Time series classification from scratch with deep neural networks: A strong baseline. In *2017 International Joint Conference on Neural Networks (IJCNN)*, pp. 1578–1585, 2017. doi: 10.1109/IJCNN.2017.7966039.

Wen, Q., Zhou, T., Zhang, C., Chen, W., Ma, Z., Yan, J., and Sun, L. Transformers in time series: A survey. In Elkind, E. (ed.), *Proceedings of the Thirty-Second International Joint Conference on Artificial Intelligence, IJCAI-23*, pp. 6778–6786. International Joint Conferences on Artificial Intelligence Organization, 8 2023. doi: 10.24963/ijcai.2023/759. URL https://doi.org/10.24963/ijcai.2023/759. Survey Track.

Woo, G., Liu, C., Kumar, A., Xiong, C., Savarese, S., and Sahoo, D. Unified training of universal time series forecasting transformers. *arXiv preprint arXiv:2402.02592*, 2024.

Wu, C.-J., Raghavendra, R., Gupta, U., Acun, B., Ardalani, N., Maeng, K., Chang, G., Behram, F. A., Huang, J., Bai, C., Gschwind, M., Gupta, A., Ott, M., Melnikov, A., Candido, S., Brooks, D., Chauhan, G., Lee, B., Lee, H.-H. S., Akyildiz, B., Balandat, M., Spisak, J., Jain, R., Rabbat, M., and Hazelwood, K. Sustainable ai: Environmental implications, challenges and opportunities, 2022.

Wu, H., Xu, J., Wang, J., and Long, M. Autoformer: Decomposition transformers with auto-correlation for long-term series forecasting. In Beygelzimer, A., Dauphin, Y., Liang, P., and Vaughan, J. W. (eds.), *Advances in Neural Information Processing Systems*, 2021. URL https://openreview.net/forum?id=I55UqU-M11y.

Wu, H., Hu, T., Liu, Y., Zhou, H., Wang, J., and Long, M. Timesnet: Temporal 2d-variation modeling for general time series analysis. In *The Eleventh International Conference on Learning Representations*, 2023. URL https://openreview.net/forum?id=ju_Uqw384Oq.

Wu, R. and Keogh, E. J. Current time series anomaly detection benchmarks are flawed and are creating the illusion of progress. *IEEE Transactions on Knowledge & Data Engineering*, 35(03):2421–2429, mar 2023. ISSN 1558-2191. doi: 10.1109/TKDE.2021.3112126.

Xie, Z., Zhang, Z., Cao, Y., Lin, Y., Bao, J., Yao, Z., Dai, Q., and Hu, H. Simmim: a simple framework for masked image modeling. In *2022 IEEE/CVF Conference on Computer Vision and Pattern Recognition (CVPR)*, pp. 9643–9653, 2022. doi: 10.1109/CVPR52688.2022.00943.

Xu, H., Chen, W., Zhao, N., Li, Z., Bu, J., Li, Z., Liu, Y., Zhao, Y., Pei, D., Feng, Y., et al. Unsupervised anomaly detection via variational auto-encoder for seasonal kpis in web applications. In *Proceedings of the 2018 world wide web conference*, pp. 187–196, 2018.

Xu, J., Wu, H., Wang, J., and Long, M. Anomaly transformer: Time series anomaly detection with association discrepancy. In *International Conference on Learning Representations*, 2022. URL https://openreview.net/forum?id=LzQQ89U1qm_.

Yue, Z., Wang, Y., Duan, J., Yang, T., Huang, C., Tong, Y., and Xu, B. Ts2vec: Towards universal representation of time series. *Proceedings of the AAAI Conference on Artificial Intelligence*, 36(8):8980–8987, Jun. 2022. doi: 10.1609/aaai.v36i8.20881. URL https://ojs.aaai.org/index.php/AAAI/article/view/20881.

Zebik, M., Korytkowski, M., Angryk, R., and Scherer, R. *Convolutional Neural Networks for Time Series Classification*, pp. 635–642. Springer International Publishing, Cham, 2017. ISBN 978-3-319-59060-8. doi: 10.1007/978-3-319-59060-8_57. URL https://doi.org/10.1007/978-3-319-59060-8_57.

Zerveas, G., Jayaraman, S., Patel, D., Bhamidipaty, A., and Eickhoff, C. A transformer-based framework for multivariate time series representation learning. In *Proceedings of the 27th ACM SIGKDD Conference on Knowledge Discovery & Data Mining*, KDD '21, pp. 2114–2124, New York, NY, USA, 2021. Association for Computing Machinery. ISBN 9781450383325. doi: 10.1145/3447548.3467401. URL https://doi.org/10.1145/3447548.3467401.

Zhou, H., Zhang, S., Peng, J., Zhang, S., Li, J., Xiong, H., and Zhang, W. Informer: Beyond efficient transformer for long sequence time-series forecasting. *Proceedings of the AAAI Conference on Artificial Intelligence*, 35(12):11106–11115, May 2021. doi: 10.1609/aaai.v35i12.17325. URL https://ojs.aaai.org/index.php/AAAI/article/view/17325.

Zhou, T., Ma, Z., Wen, Q., Wang, X., Sun, L., and Jin, R. FEDformer: Frequency enhanced decomposed transformer for long-term series forecasting. In *Proc. 39th International Conference on Machine Learning (ICML 2022)*, 2022.

Zhou, T., Niu, P., Wang, X., Sun, L., and Jin, R. One fits all: Power general time series analysis by pretrained LM. In *Thirty-seventh Conference on Neural Information Processing Systems*, 2023. URL https://openreview.net/forum?id=gMS6FVZvmF.

A. Changelog

- (Oct'2024) Added links to both research and inference benchmarks, notes on contemporary work in Tab. 9 (Timer (Liu et al., 2024) and TOTEM (Talukder et al., 2024)). We also note differences in positional embeddings (Sec. 3.2).

B. Related Work

Transformers and Patching for Time series Modeling. There is a growing body of work utilizing transformers for various time series analysis tasks, for example PatchTST (Nie et al., 2023), Informer (Zhou et al., 2021), Autoformer (Wu et al., 2021), FEDformer (Zhou et al., 2022), Pyraformer (Liu et al., 2022) for forecasting; Anomaly Transformer (Xu et al., 2022) for anomaly detection, and TST (Zerveas et al., 2021), TS-TCC (Eldele et al., 2021) for representation learning.

One issue with applying transformers to time series data is the complexity of the self-attention mechanism, which grows quadratically with the size of input tokens (or length of time series). Consequently, the primary focus of most initial applications of transformers to time series, especially for forecasting where longer look-back windows typically improve performance, was to redesign the self-attention mechanism to reduce its complexity (Zhou et al., 2021; 2022; Liu et al., 2022). Nie et al. (2023) demonstrated that treating time series sub-sequences (or patches) as tokens instead of individual time points is a simple, efficient yet effective mechanism for learning useful representations for forecasting. The authors drew inspiration from language and vision domains where sub-words (vs. characters) (Devlin et al., 2019) and 2-D patches (vs. raw pixels) (Bao et al., 2022; Dosovitskiy et al., 2021) are used as inputs to transformers. Drawing inspiration from prior work, we build on top of the transformer architecture which takes disjoint time series sub-sequences (or patches) as input.

Masked Representation Learning. Masked pre-training is a widely-used self-supervised learning task where a model learns to accurately reconstruct masked portions of its input. Masked language (Devlin et al., 2019; Raffel et al., 2020) and image modeling (Xie et al., 2022; Li et al., 2023b) have been successfully utilized to learn models from vast quantities of unlabeled data, which can generalize to a variety of downstream tasks.

For time series data, prior work has primarily focused on contrastive representation learning (Yue et al., 2022; Eldele et al., 2021; Franceschi et al., 2019). The goal of contrastive learning is to learn a representation space where "positive" pairs of time series are close while "negative" pairs are far apart. However, the notion of positive and negative pairs is subjective and data-dependent, and popular transformations such as flipping and cropping invariance may not be appropriate for time series data (Yue et al., 2022). In contrast, some studies mask portions of time series using zeros and learn a model to reconstruct them (Nie et al., 2023; Zerveas et al., 2021; Dong et al., 2023; Li et al., 2023c).

Representation learning via masking is well-suited to all the downstream tasks we care about, especially forecasting and imputation, as they are instances of the masked reconstruction problem. Owing to its simplicity and success in vision and language domains, we use the masked prediction task to pre-train our model, using a special embedding (see `[MASK]` in Fig. 3) to mask time series patches instead of zeros.

Cross-modal transfer learning using language models. Lu et al. (2022) had first shown that transformers pre-trained on text data (LLMs) can effectively solve sequence modeling tasks in other modalities. Some recent studies have leveraged this inherent ability of language pre-trained transformers to "reprogram" LLMs for time series analysis using parameter efficient fine-tuning and suitable tokenization strategies (Zhou et al., 2023; Gruver et al., 2023; Jin et al., 2023; Cao et al., 2023; Ekambaram et al., 2024). However, some of these models (Jin et al., 2023; Gruver et al., 2023) with billions of parameters demand significant memory and computational resources to perform well. We complement this line of research with three empirical observations (Sec 4.3): we show that (1) transformers trained on time series can also model sequences across modalities, (2) during pre-training, randomly initializing weights lead to lower pre-training loss, than initializing with language modeling weights, and (3) models pre-trained on time series outperform LLM-based models such as (Zhou et al., 2023; Jin et al., 2023) on many tasks and datasets.

Unanswered Questions. To the best of our knowledge, two questions remain largely unanswered in prior work on time series modeling. First, all existing time series models are (pre-)trained and fine-tuned on individual datasets (Nie et al., 2023; Yue et al., 2022; Wu et al., 2023; Zhou et al., 2023), and the benefits (or drawbacks) of large-scale multi-dataset pre-training remains unexplored (Wen et al., 2023). Second, there is very limited work on time series modeling in limited supervision settings, such as zero-shot forecasting (Oreshkin et al., 2021), or few-shot classification (Narwariya et al., 2020). In our work, we consider both these questions and *show that pre-training a model of sufficient capacity on a large corpus of unlabeled time series data can in fact enable it to provide reasonably accurate predictions in limited-supervision settings.*

C. Contemporary Work

Feature	MOMENT	Moirai	Lag-LLaMa	Chronos	Timer
Citation	Ours	(Woo et al., 2024)	(Rasul et al., 2023)	(Ansari et al., 2024)	(Liu et al., 2024)
Base Architecture	T5 encoder	Encoder-only transformer	LLaMa	T5 (encoder-decoder)	Decoder-only
Sizes	40M, 125M, 385M	14M, 91M, 311M	200M	20M, 46M, 200M, 710M	29M, 50M, 67M
Open Source	✓	✓	✓	✓	✓
Evaluation Tasks	Forecasting, Classification, Anomaly detection, Imputation	Forecasting	Forecasting	Forecasting	Forecasting, Imputation, Anomaly detection
Data Total Observations	1.13B++	27.65B[10]	0.36B[11]	84B	28B
# Time Series	13M	4M	11K	11M	7.4M
Public	✓	✓	✓	✓	✓
Public Release	May'24	Feb'2024	Feb'2024	Mar'2024	Jun'2024
Tokenization	Fixed-length patches	Multi-scale patches	Lag features	Scaling & quantization	Single-series Sequence
Objective	Reconstruction error (MSE)	Forecast log likelihood of mixture distribution	Forecast log likelihood of Student's t distribution	Forecast Cross-entropy loss	Next token prediction
Distributional Prediction	In progress (post hoc)	✓	✓	✓	×
Interpretability	✓	×	×	✓	×
Any-variate Prediction	✓ (Channel independence)	✓ (Flattening)	×	×	✓ (Uniform sub-sampling)
Context length	512	1000–5000	1024	512	1440
Scaling Model	✓	✓	✓	✓	✓
Data	×	×	✓	×	✓
Impact of Initialization	✓	×	×	✓	×

Feature	TimesFM	TimeGPT-1	TinyTimeMixers	TOTEM
Citation	(Das et al., 2023)	(Garza & Mergenthaler-Canseco, 2023)	(Ekambaram et al., 2024)	(Talukder et al., 2024)
Base Architecture	Decoder-only	Transformer	MLP-Mixer (Tolstikhin et al., 2021)	VQ-VAE (Van Den Oord et al., 2017)
Sizes	17M, 70M, 200M	?	<1M	0.3M
Open Source	×	×	✓	✓
Evaluation Tasks	Forecasting	Forecasting	Forecasting	Forecasting, Classification, Anomaly detection, Imputation
Data Total Observations	100B	100B	244M	N/A
# Time Series	?	?	N/A	N/A
Public	×	×	✓	✓
Public Release	-	-	Apr'2024	Feb'2024
Tokenization	Fixed-length patches	?	Adaptive Patching	VQVAE-based
Objective	Forecasting error (MSE)	?	Forecasting error (MSE)	Reconstruction + Commitment error
Distributional Prediction	×	✓ (post hoc)	×	✓
Interpretability	✓	×	×	×
Any-variate Prediction	×	✓ (?)	✓ (Channel Independence + Mixing)	✓ (Flattening)
Context length	512	?	512	512
Scaling Model	✓	×	✓	✓
Data	✓	×	✓	✓
Impact of Initialization	×	×	✓	×

Table 9. Time series foundation modeling has a young but growing literature. Latest ArXiv pre-prints of most contemporary work are from **February 2024** with the exception of TimeGPT-1. None of the contemporary works have evaluated their foundation models in terms of cross modal transfer, environmental impact and transparency. ++ denotes that the Time Series Pile is a living database, is still growing in size and diversity. Moirai (Woo et al., 2024) uses a mixture of Student's t, log-normal, negative binomial, and low variance normal distribution.

D. Interesting directions for future work

We note some interesting directions for future work:

- Study the impact of design choices such as the impact of the choice of the loss function (Huber, L_1, L_2), patch length $(4, 8)$, and masking percentage $(0.3, 0.6)$ on pre-training loss and time series modeling performance.

- Pre-training data. Two interesting directions include using augmentation and synthetic data (Ansari et al., 2024) to improve the quality of pre-training, and looking at tuning dataset mixtures in the Time Series Pile.

E. The Time Series Pile

We compiled a large collection of publicly available datasets from diverse domains into the Time Series Pile. It has **13** unique domains of data, which includes **20.085** GB worth of **13M** unique time series and **1.23** billion timestamps (including

channels).

Unique domains	Examples of Datasets
Healthcare	ECG, EEG, Hospital
Human Body	Tongue movement, Finger movement, Muscle Signals
Nature	Fish outlines, Flower outlines, River flow
Audio	Arabic speech, Japanese Speech, Phonetics
Power	Power consumption, Electricity, Home appliance usage
Economics	Exchange Rate, Bitcoin, Tourism
Traffic	Road Traffic, Pedestrian cross, Line occupancy rate
Weather	Temperature, Rain, Wind
Facilities	Machine Status, Spacecraft Status, Web traffic
Web Services	IOPS, NAB
Synthetic	MGAB
Sensors	NASA MSL, NASA SMAP
Gait	Daphnet

Table 10. **The Time Series Pile** covers datasets from 13 distinct domains.

Task	Dataset	Channels	Series Length	Data Size (Train, Val, Test)	Information (Frequency/Number of Classes)
Long horizon forecasting (Informer)	ETTm1, ETTm2	7	{96, 720}	(33953, 11425, 11425)	Electricity (15 mins)
	ETTh1, ETTh2	7		(8033, 2785, 2785)	Electricity (15 mins)
	Electricity	321		(17805, 2537, 5165)	Electricity (Hourly)
	Traffic	862		(11673, 1661, 3413)	Transportation (Hourly)
	Weather	21		(36280, 5175, 10444)	Weather (10 mins)
	Exchange	8		(4704, 665, 1422)	Exchange rate (Daily)
	ILI	7	{24, 60}	(69, 2, 98)	Illness (Weekly)
Short horizon forecasting (Monash)	M4-Yearly	1	6	(16099, 2301, 4600)	-
	M4-Quarterly		8	(16800, 2400, 4800)	-
	M4-Monthly		18	(33600, 4800, 9600)	-
	M3-Yearly		6	(451, 65, 129)	-
	M3-Quarterly		8	(529, 76, 151)	-
	M3-Monthly		18	(999, 144, 285)	-
Imputation (Informer)	ETTm1, ETTm2	7	512	(33953, 11425, 11425)	Electricity (15 mins)
	ETTh1, ETTh2	7		(8033, 2785, 2785)	Electricity (15 mins)
	Electricity	321		(17805, 2537, 5165)	Electricity (Hourly)
	Weather	21		(36280, 5175, 10444)	Weather (10 mins)
Classification (UCR)	UWaveGestureLibraryX	1	315	(640, 256, 3582)	Motion Gesture (8 classes)
	ECG5000		140	(357, 143, 4500)	ECG Record (5 classes)
	OSULeaf		427	(142, 58, 242)	Leaf Outlines (6 classes)
	MedicalImages		99	(272, 109, 760)	Pixel Intensity (10 classes)
	Ham		431	(77, 32, 105)	Food spectrographs (2 classes)
Anomaly detection (TSB-UAD)	1sddb40	1	-	(24489, 9489, 3969)	Beats
	BIDMC1		-	(1274, 204, 7988)	PVC
	CIMIS44AirTemperature3		-	(2346, 632, 3672)	Weather Data
	CIMIS44AirTemperature5		-	(2346, 632, 3672)	Weather Data
	ECG2		-	(10203, 3775, 14488)	ECG2 Lead

Table 11. **Subset of The Time Series Pile used for experiments.** A brief description of datasets that collectively make the Time Series Pile. Due to space constraints, we only include metadata for the subsets of the M3 and M4 datasets in our experiments, as well as 5 classification and anomaly detection datasets. Characteristics of all short-horizon forecasting, classification and anomaly detection datasets in the Time Series Pile can be found in our official repository, and Monash archive, UCR/UEA classification archive, and TSB-UAD anomaly benchmark, respectively.

Dataset	Domain	# time series	Min Length	Mean Length	Max Length	Total Observations	Average # of anomalies	Average # of abnormal points
Dodger	Traffic	1	50399	50399	50399	50399	133	5612
ECG	Healthcare	74	5000	311189.82	10828799	23028047	195.6	15634
IOPS	Web Services	29	7577	100648.89	149160	2918818	46.5	2312.3
KDD21	Multiple	250	1000	21215.04	250000	5303761	1	196.5
MGAB	Synthetic	10	99999	99999	99999	999990	10	200
NAB	Web Services	58	1125	6300.72	22693	365442	2	575.5
SensorScope	Weather	23	20732	27037.43	30492	621861	11.2	6110.4
YAHOO	Web Services	367	740	1560.21	1679	572599	5.9	10.7
NASA-MSL	Sensors	27	438	2158.88	4307	58290	1.33	286.3
NASA-SMAP	Sensors	54	311	2554.62	2880	137950	1.26	1032.4
Daphnet	Gait	45	9599	21759	55039	979155	7.6	2841
GHL	Sensors	126	200000	200000	200000	25200000	1.2	388.8
Genesis	Sensors	6	16219	16219	16219	97314	3	50
MITDB	Healthcare	32	649999	649999	649999	20799968	210.1	72334.3
OPP	Sensors	465	22229	31615.85	51115	14701373	2	1267.3
Occupancy	Sensors	7	2664	4688.85	9751	32822	18.3	1414.5
SMD	Web Services	281	23686	25561.30	28742	7182727	10.4	900.2
SVDB	Healthcare	115	230399	230399	230399	26495885	208	27144.5

Table 12. **Anomaly detection datasets in Time Series Pile taken from (Paparrizos et al., 2022b).** The total number of observations is **129,546,401**, while the total number of unique time series is **1,970**.

Dataset	Domain	# Time-series	# Classes	# Channels	Time Series Length	# Time Series (w. channels)	Total Observations
SemgHandGenderCh2	Human Body	900	2	1	1500	900	1350000
GestureMidAirD2	Human Body	338	26	1	360	338	121680
UWaveGestureLibraryAll	Human Body	4478	8	1	945	4478	4231710
SelfRegulationSCP1	Healthcare	561	2	6	896	3366	3015936
UWaveGestureLibraryX	Human Body	4478	8	1	315	4478	1410570
GesturePebbleZ2	Human Body	304	6	1	455	304	138320
Healthcare5000	Healthcare	5000	5	1	140	5000	700000
OSULeaf	Nature	442	6	1	427	442	188734
MedicalImages	Healthcare	1141	10	1	99	1141	112959
Haptics	Human Body	463	5	1	1092	463	505596
LargeKitchenAppliances	Power	750	3	1	720	750	540000
JapaneseVowels	Audio	640	9	12	26	7680	199680
Worms	Nature	258	5	1	900	258	232200
Ham	Facilities	214	2	1	431	214	92234
DistalPhalanxTW	Nature	539	6	1	80	539	43120
ProximalPhalanxOutlineCorrect	Nature	891	2	1	80	891	71280
SemgHandMovementCh2	Human Body	900	6	1	1500	900	1350000
RefrigerationDevices	Power	750	3	1	720	750	540000
FreezerRegularTrain	Facilities	3000	2	1	301	3000	903000
PigAirwayPressure	Nature	312	52	1	2000	312	624000
TwoLeadECG	Healthcare	1162	2	1	82	1162	95284
GunPointMaleVersusFemale	Human Body	451	2	1	150	451	67650
Trace	Power	200	4	1	275	200	55000
SmoothSubspace	Generated	300	3	1	15	300	4500
MiddlePhalanxTW	Nature	553	6	1	80	553	44240
AtrialFibrillation	Healthcare	30	3	2	640	60	38400
SyntheticControl	Generated	600	6	1	60	600	36000
ShapesAll	Generated	1200	60	1	512	1200	614400
Human BodyVerticalSignal	Human Body	724	12	1	1250	724	905000
PLAID	Facilities	1074	11	1	1344	1074	1443456
AllGestureWiimoteX	Human Body	1000	10	1	385	1000	385000
Heartbeat	Healthcare	409	2	61	405	24949	10104345
Wafer	Facilities	7164	2	1	152	7164	1088928
FaceFour	Generated	112	4	1	350	112	39200
Phoneme	Audio	2110	39	1	1024	2110	2160640
InlineSkate	Human Body	650	7	1	1882	650	1223300

CricketX	Human Body	780	12	1	300	780	234000
SelfRegulationSCP2	Healthcare	380	2	7	1152	2660	3064320
DistalPhalanxOutlineCorrect	Nature	876	2	1	80	876	70080
ChlorineConcentration	Nature	4307	3	1	166	4307	714962
Chinatown	Traffic	363	2	1	24	363	8712
GestureMidAirD1	Human Body	338	26	1	360	338	121680
MiddlePhalanxOutlineAgeGroup	Nature	554	3	1	80	554	44320
UMD	Generated	180	3	1	150	180	27000
Crop	Nature	24000	24	1	46	24000	1104000
PenDigits	Facilities	10992	10	2	8	21984	175872
GesturePebbleZ1	Human Body	304	6	1	455	304	138320
Handwriting	Facilities	1000	26	3	152	3000	456000
Mallat	Generated	2400	8	1	1024	2400	2457600
ERing	Human Body	300	6	4	65	1200	78000
StarLightCurves	Nature	9236	3	1	1024	9236	9457664
WordSynonyms	Audio	905	25	1	270	905	244350
PEMS-SF	Traffic	440	7	963	144	423720	61015680
FaceDetection	Human Body	9414	2	144	62	1355616	84048192
Computers	Power	500	2	1	720	500	360000
ArrowHead	Generated	211	3	1	251	211	52961
Wine	Nature	111	2	1	234	111	25974
Coffee	Nature	56	2	1	286	56	16016
Earthquakes	Nature	461	2	1	512	461	236032
Herring	Nature	128	2	1	512	128	65536
Lightning2	Nature	121	2	1	637	121	77077
Beef	Nature	60	5	1	470	60	28200
MiddlePhalanxOutlineCorrect	Nature	891	2	1	80	891	71280
HealthcareFiveDays	Healthcare	884	2	1	136	884	120224
Yoga	Human Body	3300	2	1	426	3300	1405800
Adiac	Nature	781	37	1	176	781	137456
HandMovementDirection	Human Body	234	4	10	400	2340	936000
MoteStrain	Facilities	1272	2	1	84	1272	106848
Rock	Nature	70	4	1	2844	70	199080
Strawberry	Nature	983	2	1	235	983	231005
InsectWingbeatSound	Nature	2200	11	1	256	2200	563200
DodgerLoopWeekend	Traffic	158	2	1	288	158	45504
MixedShapesSmallTrain	Generated	2525	5	1	1024	2525	2585600
EthanolConcentration	Power	524	4	3	1751	1572	2752572
OliveOil	Nature	60	4	1	570	60	34200
Meat	Nature	120	3	1	448	120	53760
MelbournePedestrian	Traffic	3633	10	1	24	3633	87192
Car	Facilities	120	4	1	577	120	69240
FaceAll	Human Body	2250	14	1	131	2250	294750
FacesUCR	Human Body	2250	14	1	131	2250	294750
AllGestureWiimoteY	Human Body	1000	10	1	369	1000	369000
NATOPS	Human Body	360	6	24	51	8640	440640
SemgHandSubjectCh2	Human Body	900	5	1	1500	900	1350000
ShakeGestureWiimoteZ	Human Body	100	10	1	385	100	38500
Cricket	Human Body	180	12	6	1197	1080	1292760
BME	Generated	180	3	1	128	180	23040
EigenWorms	Nature	259	5	6	17984	1554	27947136
FordB	Facilities	4446	2	1	500	4446	2223000
NonInvasiveFetalHealthcareThorax1	Healthcare	3765	42	1	750	3765	2823750
UWaveGestureLibrary	Human Body	440	8	3	315	1320	415800
CinCHealthcareTorso	Healthcare	1420	4	1	1639	1420	2327380
PigArtPressure	Nature	312	52	1	2000	312	624000
Fish	Nature	350	7	1	463	350	162050
SonyAIBORobotSurface2	Facilities	980	2	1	65	980	63700
FiftyWords	Facilities	905	50	1	270	905	244350
MotorImagery	Healthcare	378	2	64	3000	24192	72576000
ToeSegmentation1	Human Body	268	2	1	277	268	74236
PhonemeSpectra	Audio	6668	39	11	217	73348	15916516
FreezerSmallTrain	Facilities	2878	2	1	301	2878	866278
TwoPatterns	Generated	5000	4	1	128	5000	640000
ShapeletSim	Generated	200	2	1	500	200	100000

Plane	Generated	210	7	1	144	210	30240
GestureMidAirD3	Human Body	338	26	1	360	338	121680
DiatomSizeReduction	Generated	322	4	1	345	322	111090
Human BodyHorizontalSignal	Human Body	724	12	1	1250	724	905000
CricketZ	Human Body	780	12	1	300	780	234000
StandWalkJump	Human Body	27	3	4	2500	108	270000
WormsTwoClass	Human Body	258	2	1	900	258	232200
Lightning7	Nature	143	7	1	319	143	45617
UWaveGestureLibraryY	Human Body	4478	8	1	315	4478	1410570
GunPointAgeSpan	Human Body	451	2	1	150	451	67650
DistalPhalanxOutlineAgeGroup	Nature	539	3	1	80	539	43120
SwedishLeaf	Nature	1125	15	1	128	1125	144000
LSST	Nature	4925	14	6	36	29550	1063800
CBF	Generated	930	3	1	128	930	119040
BeetleFly	Nature	40	2	1	512	40	20480
Libras	Human Body	360	15	2	45	720	32400
HouseTwenty	Facilities	159	2	1	2000	159	318000
ScreenType	Facilities	750	3	1	720	750	540000
InsectEPGSmallTrain	Nature	266	3	1	601	266	159866
AllGestureWiimoteZ	Sensor	1000	10	1	326	1000	326000
DodgerLoopDay	Sensor	158	7	1	288	158	45504
NonInvasiveFetalHealthcareThorax2	Healthcare	3765	42	1	750	3765	2823750
BasicHuman Bodys	Human Body	80	4	6	100	480	48000
GunPointOldVersusYoung	Human Body	451	2	1	150	451	67650
FordA	Sensor	4921	2	1	500	4921	2460500
InsectWingbeat	Nature	50000	10	200	22	10000000	220000000
ItalyPowerDemand	Power	1096	2	1	24	1096	26304
ProximalPhalanxOutlineAgeGroup	Nature	605	3	1	80	605	48400
ACSF1	Power	200	10	1	1460	200	292000
GunPoint	Human Body	200	2	1	150	200	30000
RacketSports	Human Body	303	4	6	30	1818	54540
SmallKitchenAppliances	Power	750	3	1	720	750	540000
ProximalPhalanxTW	Nature	605	6	1	80	605	48400
DuckDuckGeese	Facilities	100	5	1345	270	134500	36315000
PickupGestureWiimoteZ	Human Body	100	10	1	361	100	36100
EthanolLevel	Power	1004	4	1	1751	1004	1758004
SpokenArabicDigits	Audio	8798	10	13	93	114374	10636782
SonyAIBORobotSurface1	Facilities	621	2	1	70	621	43470
HandOutlines	Human Body	1370	2	1	2709	1370	3711330
PowerCons	Power	360	2	1	144	360	51840
PhalangesOutlinesCorrect	Nature	2658	2	1	80	2658	212640
BirdChicken	Nature	40	2	1	512	40	20480
ToeSegmentation2	Human Body	166	2	1	343	166	56938
PigCVP	Healthcare	312	52	1	2000	312	624000
CricketY	Human Body	780	12	1	300	780	234000
FingerMovements	Human Body	416	2	28	50	11648	582400
ElectricDevices	Power	16637	7	1	96	16637	1597152
InsectEPGRegularTrain	Nature	311	3	1	601	311	186911
DodgerLoopGame	Traffic	158	2	1	288	158	45504
Fungi	Nature	204	18	1	201	204	41004
Symbols	Generated	1020	6	1	398	1020	405960
MixedShapesRegularTrain	Generated	2925	5	1	1024	2925	2995200
ArticularyWordRecognition	Human Body	575	25	9	144	5175	745200
UWaveGestureLibraryZ	Human Body	4478	8	1	315	4478	1410570
Epilepsy	Human Body	275	4	3	206	825	169950
Healthcare200	Healthcare	200	2	1	96	200	19200

Table 16: **Classification datasets in Time Series Pile taken from (Ismail Fawaz et al., 2019) [UCR Archive].** The total number of observations is 634,084,943, while the total number of unique time series is 290,226.

F. Experimental Setup and Results

Through our experiments, our goal is to answer the following research questions.

Dataset	Domain	# Time Series	Min Length	Mean Length	Max Length	Total Observations	Frequency	Forecast Horizon
Australian Electricity Demand	Power	5	230736	231052.8	232272	1155264	Half Hourly	
Bitcoin	Economics	18	2659	4186.88	4581	75364	Daily	
Car Parts	Economics	2674	51	51	51	136374	monthly	
CIF 2016	Economics	72	28	98.72	120	7108	monthly	
Covid Deaths	Nature	266	212	212	212	56392	Daily	
Dominick	Economics	115704	28	165.01	393	19092987	weekly	
Electricity	Power	321	26304	26304	26304	8443584	hourly	
		321	156	156	156	50076	weekly	8
FRED MD	Economics	107	728	728	728	77896	monthly	
Hospital	Healthcare	767	84	84	84	64428	monthly	
Kaggle Web Traffic	Web Services	145063	803	803	803	116485589	Daily	59
		145063	114	114	114	16537182	weekly	8
KDD Cup 2028	Nature	270	9504	10897.64	10920	2942364	hourly	
London Smart Meters	Power	5560	288	29951.24	39648	166528896	half_hourly	
M1	Multiple	617	48	90.75	150	55998	monthly	18
		203	18	48.98	114	9944	quarterly	8
		181	15	24.94	58	4515	yearly	6
M3	Multiple	1428	66	117.34	144	167562	monthly	18
		174	71	76.58	104	13325		8
		756	24	48.94	72	37004	quarterly	8
		645	20	28.40	47	18319	yearly	6
M4	Multiple	4227	107	2371.38	9933	10023836	daily	14
		414	748	901.86	1008	373372	hourly	48
		48000	60	234.30	2812	11246411	monthly	18
		24000	24	100.25	874	2406108	quarterly	8
		359	93	1035.03	2610	371579	weekly	13
		23000	19	37.32	841	858458	yearly	6
NN5	Economics	111	791	791	791	87801	daily	56
		111	113	113	113	12543	weekly	8
Pedestrian Counts	Traffic	66	576	47459.78	96424	3132346	hourly	
Rideshare	Traffic	2304	541	541	541	1246464	hourly	
Saugeenday	Nature	1	23741	23741	23741	23741	daily	
Solar	Power	137	52560	52560	52560	7200720	10_minutes	
		1	7397222	7397222	7397222	7397222	4_seconds	
		137	52	52	52	7124	weekly	5
Sunspot	Nature	1	73931	73931	73931	73931	daily	
Temperature Rain	Nature	32072	725	725	725	23252200	daily	
Tourism	Economics	366	91	298.57	333	109280	monthly	24
		427	30	99.63	130	42544	quarterly	8
		518	11	24.62	47	12757	yearly	4
Traffic	Traffic	862	17544	17544	17544	15122928	hourly	
		862	104	104	104	89648	weekly	8
US Births	Nature	1	7305	7305	7305	7305	daily	
Vehicle Trips	Traffic	329	70	128.82	243	42544	daily	
Weather	Weather	3010	1332	14296.34	65981	43032000	daily	
Wind	Power	1	7397147	7397147	7397147	7397147	4_seconds	
Wind Farms	Power	339	6345	507899.88	527040	172178060	minutely	

Table 13. **Short horizon forecasting datasets in Time Series Pile** taken from (Godahewa et al., 2021). The total number of observations is **281,326,601**, while the total number of unique time series is **559,102**.

Dataset	Domain	# Time Series	Min Length	Mean Length	Max Length	Total Observations	Frequency	Forecast Horizon
		464	791	1570.08	25289	728520	Daily	14
		188028	19	34.76	339	6535989	Yearly	6
FRED	Economics	1630	94	1261.12	5396	2055634	Weekly	13
		133411	60	302.49	3867	40356476	Monthly	18
		58908	24	120.11	1288	7075821	Quarterly	8

Table 14. **Short horizon forecasting dataset in Time Series Pile** taken from the Federal Reserve Economic Data [(FRED)] (Oreshkin et al., 2021). The total number of observations is **56,752,440**, while the total number of unique time series is **382,441**.

Is MOMENT effective for multiple time series analysis tasks in limited and rich supervision settings? We conduct large-scale experiments on widely used benchmarks to evaluate MOMENT on forecasting, classification, anomaly detection, and imputation as outlined in Table 8. The *limited supervision* setting mimics practical scenarios in which it is infeasible to train (or fine-tune) a deep

Dataset	Domain	# Channels	Time Series Length	Total Observations	Frequency	Forecast Horizon
Electricity	Power	321	26304	8443584	Hourly	{96, 192, 336, 720}
ETTh1	Power	7	17420	121940	Hourly	{96, 192, 336, 720}
ETTh2	Power	7	17420	121940	Hourly	{96, 192, 336, 720}
ETTm1	Power	7	69680	487760	15 Minute	{96, 192, 336, 720}
ETTm2	Power	7	69680	487760	15 Minute	{96, 192, 336, 720}
Exchange	Finance	8	7588	60704	Daily	{96, 192, 336, 720}
Illness	Epidemiology	7	966	6762	Weekly	{24, 36, 48, 60}
Traffic	Traffic	862	17544	15122928	Hourly	{96, 192, 336, 720}
Weather	Weather	21	52696	1106616	10 Minute	{96, 192, 336, 720}

Table 15. **Long-horizon forecasting datasets in the Time Series Pile taken from Zhou et al. (2021)**. The total number of observations is **25,959,994**, while the total number of unique time series is **1,247**.

neural network due to limited compute and, little or inadequately characterized data. In these settings, MOMENT provides predictions without any explicit (re)training on target data[12]. On the other hand, the rich supervision setting allows us to examine whether MOMENT can utilize task-specific data to improve its performance via end-to-end fine-tuning or linear probing.

What does MOMENT learn? We evaluated MOMENT's ability to model time series characteristics such as varying frequencies, trends, and scales. Structure in the PCA and t-SNE (Fig. 9) visualizations of the embeddings of synthetically generated sinusoids suggest that MOMENT can capture subtle trend, scale, frequency, and auto-correlation information. ϵ denotes gaussian noise with 0 mean and 0.1 standard deviation. c controls the factor of interest, i.e. the power of the trend polynomial, amplitude, and frequency of the sine waves in experiments (i), (ii) & (iii), respectively.

Hyper-parameter Tuning. We do not perform extensive hyper-parameter tuning. In all experiments that follow, unless mentioned otherwise, we fine-tune MOMENT-Base with a batch size of 16, and cosine learning rate schedule with an initial learning rate of $1e^{-5}$. For baseline methods, we capture recommended settings from their respective papers and public repositories. We report all hyper-parameters settings for MOMENT and baselines in Appendix D.

F.1. Forecasting

Task description. Given a time series $\mathcal{T} = [x_1, ..., x_L]$ where $x_i \in \mathbb{R}$, the univariate forecasting problem is to predict the next H time-steps $[x_{L+1}, ..., x_{L+H}]$. Depending on the length of the horizon, forecasting can be categorized as *short* or *long-horizon*[13]. We consider both tasks in our experiments. We propose two configurations of MOMENT for the forecasting problem: (1) we can produce short-horizon forecasts without any explicit training or fine-tuning, by appending masked patches and predicting them using the default reconstruction head (Fig. 4 (ii)); (2) alternatively, we can replace the reconstruction head to a forecasting head and then fine-tune it (Fig. 4 (i)).

F.1.1. LONG-HORIZON FORECASTING

Datasets. We use all the long-horizon forecasting datasets (Sec 3.1). But to speed up our experiments, we drop all exogenous variables from multi-variate datasets and only consider the target time series for forecasting.

Baselines. We compare our methods with various transformer-based and deep learning baselines. These models can be found in Table 18. For Time-LLM we could not run experiments on Weather, electricity, and traffic datasets, due to time constraints, and since we could not fit them into a single GPU.

Experimental Setting. We train all models with a look-back window of length $L = 512$ to forecast $T = 24, 60$ time-steps for the ILI dataset and $T = 96, 720$ for the rest. We evaluate the Mean Squared Error (MSE) and Mean Absolute Error (MAE) as metrics.

Hyperparameters. The hyperparameters used for training all models in our long-horizon forecasting experiments are shown in Table 17.

---

[12]For classification, the quality of MOMENT's representations is measured using the accuracy of a Support Vector Machine trained on them, as is common in prior work on unsupervised representation learning (Yue et al., 2022; Franceschi et al., 2019). However, unlike prior work, MOMENT embeds time series without any data-specific training.

[13]The distinction between long and short-horizon forecasting is rather arbitrary. For instance, most of the default forecasting horizons for the long-horizon forecasting benchmark Influenza-like Illness (24, 36, 48, 60) are shorter than the Hourly subset of the M4 dataset, a popular short-horizon forecasting benchmark.

Model	Hyper-parameters	
MOMENT	sequence length:	512
	patch length:	8
	patch stride length:	8
	initial learning rate:	0.0001
	forecast horizon:	{96, 720}
Time-LLM	sequence length:	512
	patch length:	16
	patch stride length:	8
	initial learning rate:	0.001
	dimension of feedforward layer:	2048
	llm layers:	32
	number of heads:	8
N-BEATS	sequence length:	512
	stack types:	{trend, seasonality}
	number of blocks per stack:	3
	thetas dimensions:	{4, 8}
	hidden layer units:	256

Table 17. Hyper-parameter values for long-horizon forecasting models.

Methods	MOMENT_{LP}		Time-LLM		GPT4TS		PatchTST		DLinear		TimesNet		FEDformer		Pyraformer		Autoformer		Stationary		ETSformer		LightTS		Informer		Reformer		LogTrans		N-BEATS	
Metric	MSE	MAE	MSE	MAE	MSE	MAE	MSE	MAE	MSE	MAE	MSE	MAE	MSE	MAE	MSE	MAE	MSE	MAE	MSE	MAE	MSE	MAE	MSE	MAE	MSE	MAE	MSE	MAE	MSE	MAE	MSE	MAE
Weather 96	0.154	0.209	-	-	0.162	0.212	0.149	0.198	0.176	0.237	0.172	0.220	0.217	0.296	0.896	0.556	0.266	0.336	0.173	0.223	0.197	0.281	0.182	0.242	0.300	0.384	0.689	0.596	0.458	0.490	0.152	0.210
Weather 720	0.315	0.336	-	-	0.326	0.337	0.314	0.334	0.333	0.362	0.365	0.359	0.403	0.428	1.004	0.934	0.419	0.428	0.414	0.410	0.352	0.288	0.352	0.386	1.059	0.741	1.130	0.792	0.869	0.675	0.331	0.359
ETTh1 96	0.387	0.410	0.408	0.429	0.376	0.397	0.370	0.399	0.375	0.399	0.384	0.402	0.376	0.419	0.664	0.612	0.449	0.459	0.513	0.491	0.494	0.479	0.424	0.432	0.865	0.713	0.837	0.728	0.878	0.740	0.399	0.428
ETTh1 720	0.454	0.472	0.523	0.514	0.477	0.456	0.447	0.466	0.472	0.490	0.521	0.500	0.506	0.507	0.963	0.782	0.514	0.512	0.643	0.616	0.562	0.535	0.547	0.533	1.181	0.865	1.257	0.889	1.135	0.852	0.608	0.573
ETTh2 96	0.288	0.345	0.285	0.348	0.285	0.342	0.274	0.336	0.289	0.353	0.340	0.374	0.358	0.397	0.645	0.597	0.346	0.388	0.476	0.458	0.340	0.391	0.397	0.437	3.755	1.525	2.626	1.317	2.116	1.197	0.327	0.387
ETTh2 720	0.403	0.439	0.399	0.435	0.406	0.441	0.379	0.422	0.605	0.551	0.462	0.468	0.463	0.474	0.963	0.783	0.515	0.511	0.562	0.560	0.500	0.497	0.863	0.672	3.647	1.625	3.874	1.697	3.188	1.540	1.454	0.847
ETTm1 96	0.293	0.349	0.384	0.403	0.292	0.346	0.290	0.342	0.299	0.343	0.338	0.375	0.379	0.419	0.543	0.510	0.505	0.475	0.386	0.398	0.375	0.398	0.374	0.400	0.672	0.571	0.538	0.528	0.600	0.546	0.318	0.367
ETTm1 720	0.405	0.416	0.437	0.429	0.417	0.421	0.416	0.420	0.425	0.421	0.478	0.450	0.543	0.490	0.908	0.724	0.671	0.561	0.585	0.516	0.499	0.462	0.527	0.502	1.166	0.823	1.102	0.841	1.153	0.820	0.448	0.448
ETTm2 96	0.170	0.260	0.181	0.269	0.173	0.262	0.165	0.255	0.167	0.269	0.187	0.267	0.203	0.287	0.435	0.507	0.255	0.339	0.192	0.274	0.189	0.280	0.209	0.308	0.365	0.453	0.658	0.619	0.768	0.642	0.197	0.271
ETTm2 720	0.363	0.387	0.366	0.388	0.378	0.401	0.362	0.385	0.397	0.421	0.408	0.403	0.421	0.415	3.625	1.451	0.433	0.432	0.417	0.413	0.414	0.413	0.675	0.587	3.379	1.338	2.631	1.242	3.048	1.328	0.395	0.419
ILI 24	2.728	1.114	3.025	1.195	2.063	0.881	1.319	0.754	2.215	1.081	2.317	0.934	3.228	1.260	1.420	2.012	3.483	1.287	2.294	0.945	2.527	1.020	8.313	2.144	5.764	1.677	4.400	1.382	4.480	1.444	4.539	1.528
ILI 60	2.893	1.132	3.245	1.221	1.979	0.957	1.470	0.788	2.368	1.096	2.027	0.928	2.857	1.157	7.662	2.100	2.770	1.125	2.178	0.963	2.487	1.016	7.283	1.985	5.264	1.564	4.882	1.483	5.278	1.560	5.429	1.661
ECL 96	0.138	0.242	-	-	0.139	0.238	0.129	0.222	0.140	0.237	0.168	0.272	0.193	0.308	0.386	0.449	0.201	0.317	0.169	0.273	0.187	0.304	0.207	0.307	0.274	0.368	0.312	0.402	0.258	0.357	0.131	0.228
ECL 720	0.211	0.305	-	-	0.206	0.297	0.197	0.290	0.203	0.301	0.220	0.320	0.246	0.355	0.376	0.445	0.254	0.361	0.222	0.321	0.233	0.345	0.265	0.360	0.373	0.439	0.340	0.420	0.283	0.376	0.208	0.298
Traffic 96	0.391	0.282	-	-	0.388	0.282	0.360	0.249	0.410	0.282	0.593	0.321	0.587	0.366	2.085	0.468	0.613	0.388	0.612	0.338	0.607	0.392	0.615	0.391	0.719	0.391	0.732	0.423	0.684	0.384	0.375	0.259
Traffic 720	0.450	0.310	-	-	0.450	0.312	0.432	0.286	0.466	0.315	0.640	0.350	0.626	0.382	0.881	0.473	0.660	0.408	0.653	0.355	0.632	0.396	0.658	0.407	0.864	0.472	0.755	0.423	0.717	0.396	0.508	0.335

Table 18. Long-term forecasting performance measured using Mean Squared Error (MSE) and Mean Absolute Error (MAE).

Models		MOMENT		iTransformer		RLinear		PatchTST		Crossformer		TiDE		TimesNet		DLinear		SCINet		FEDFormer		Stationary		Autoformer	
Dataset	Pred_horizon	MSE	MAE	MSE	MAE	MSE	MAE	MSE	MAE	MSE	MAE	MSE	MAE	MSE	MAE	MSE	MAE	MSE	MAE	MSE	MAE	MSE	MAE	MSE	MAE
PEMS08	12	0.132	0.249	0.079	0.182	0.133	0.247	0.168	0.232	0.165	0.214	0.227	0.343	0.112	0.212	0.154	0.276	0.087	0.184	0.173	0.273	0.109	0.207	0.436	0.485
	24	0.212	0.320	0.115	0.219	0.249	0.343	0.224	0.281	0.215	0.260	0.318	0.409	0.141	0.238	0.248	0.353	0.122	0.221	0.210	0.301	0.140	0.236	0.467	0.502
	36	0.309	0.393	0.186	0.235	0.569	0.544	0.321	0.354	0.315	0.355	0.497	0.510	0.198	0.283	0.440	0.470	0.189	0.270	0.320	0.394	0.211	0.294	0.966	0.733

Table 19. Long-term forecasting performance with a look-back window of 96 time-steps. Results are taken from iTransformer (Liu et al., 2023).

F.1.2. ZERO-SHOT SHORT-HORIZON FORECASTING

Datasets. To evaluate zero-shot forecasting performance, we conduct experiments on the M3 and M4 datasets (Sec. 3.1).

Baselines. We compare MOMENT with GPT4TS (Zhou et al., 2023), TimesNet (Wu et al., 2023), N-BEATS (Oreshkin et al., 2020), 3 statistical and 3 benchmarking forecasting methods: AutoARIMA, AutoTheta, AutoETS, Naive, Seasonal Naive, and Random Walk (Makridakis et al., 2020).

Experimental Setting. Each statistical method is *fit* on individual time series before producing a forecast. We follow the same train-test split and forecasting horizons from the M3 and M4 competitions, and report sMAPE as is common in prior work (Oreshkin et al., 2020; Wu et al., 2023)[14]. We follow the same experimental procedure as outlined in (Oreshkin et al., 2021) with two exceptions: our results are reported only (1) on 40% of the M3 and M4 datasets that were unseen during pre-training, (2) a subset of frequencies with largest support in the datasets. Daily, hourly, and weekly frequencies had very little data and we could not get promising zero-shot performance for any of the deep learning models. Some ways that prior work (Oreshkin et al., 2021) had overcome this issue was by leveraging data from frequencies with plenty of data. We also believe that ensembling played an important part in N-BEATS promising zero-shot performance.

Hyperparameters. The hyperparameters used for training all models in our short-horizon forecasting experiments are shown in Table 20.

---

[14]The definitions of sMAPE were different in the M3 and M4 competitions. In our experiments, we used the same definition as the M4 competition.

Model	Hyper-parameters	
MOMENT$_{\text{LP}}$	sequence length:	512
	patch length:	8
	patch stride length:	8
	initial learning rate:	0.002
	max epochs:	$\{5, 10\}$
MOMENT$_0$	sequence length:	512
	patch length:	8
	patch stride length:	8
	initial learning rate:	0.001
N-BEATS	sequence length:	512
	stack types:	$\{$'trend', 'seasonality'$\}$
	number of blocks per stack:	3
	thetas dimensions:	$\{4, 8\}$
	hidden layer units:	256
GPT4TS	forecast horizon:	0
	gpt layers:	3
	patch length:	1
	patch stride length:	1
	sequence length:	512
TimesNet	sequence length:	512
	model dimension:	32
	dimension of feedforward layer:	32
	top-k:	5

Table 20. Hyper-parameter values for short-horizon forecasting models.

Source Dataset → Target Dataset ↓	M4	Fred
M4		
Yearly	-	Yearly
Quarterly	-	Quarterly
Monthly	-	Monthly
M3		
Yearly	Yearly	Yearly
Quarterly	Quarterly	Quarterly
Monthly	Monthly	Monthly

Table 21. Experimental settings for short-horizon forecasting experiments for varying source and target datasets.

F.2. Classification

Task Description. The classification problem comprises of learning a mapping $f : \mathcal{T} \rightarrow \{1, ..., C\}$ from a time series to a finite set of classes, using a training dataset of the form $\{(\mathcal{T}_0, c_0), ..., (\mathcal{T}_n, c_n)\}$, $c_i \in \{1, ..., C\}$. One straightforward way to use MOMENT to learn f is to replace its reconstruction head with a linear head that maps patch representations to the C logits. Another way would be to learn f in two stages, as is common in prior work on unsupervised representation learning (Yue et al., 2022; Franceschi et al., 2019): in the first stage, we obtain sequence-level representations for each time series without access to labels. The second stage involves learning any ML classifier (e.g., Support Vector Machine with RBF kernel) using these representations and labels.

Datasets. We conduct experiments on a subset of 95 datasets from the UCR Classification Archive (Dau et al., 2018). These datasets (listed in Table 10) comprise of equal-length univariate time series shorter than 512 time steps.

Baselines. We compare MOMENT against 5 **unsupervised representation learning** methods (TS2Vec (Yue et al., 2022), TST (Zerveas et al., 2021), TS-TCC (Eldele et al., 2021), TNC (Tonekaboni et al., 2021), and T-Loss (Franceschi et al., 2019)), 8 **supervised deep learning** (CNN (Zebik et al., 2017), Encoder (Serrà et al., 2018), FCN (Wang et al., 2017), MCNN (Cui et al., 2016), MLP (Wang et al., 2017), ResNet (Wang et al., 2017), t-LeNet (Le Guennec et al., 2016), TWIESN (Tanisaro & Heidemann, 2016)), 1 **supervised statistical learning** method DTW (Dau et al., 2018)), TimesNet (Wu et al., 2023) and GPT4TS (Zhou et al., 2023).

Experimental Setting. All models except for MOMENT were trained on each dataset individually, either with labels for supervised deep and statistical learning methods), or without labels for representation learning methods. We collect baseline results for deep learning methods from Ismail Fawaz et al. (2019), representation learning methods from Yue et al. (2022), and DTW from Dau et al. (2018). We

Model name / Dataset name	Adjusted Best F_1						VUS-ROC					
	Anomaly Transformer	MOMENT_0	MOMENT_{LP}	DGHL	GPT4TS	TimesNet	AnomalyTransformer	MOMENT_0	MOMENT_{LP}	DGHL	GPT4TS	TimesNet
1sddb40	0.030	0.560	0.540	0.390	0.190	0.680	0.640	0.740	0.750	0.640	0.660	0.720
BIDMC1	0.990	1.000	1.000	1.000	1.000	1.000	0.690	0.560	0.650	0.720	0.630	0.740
CHARISfive	0.010	0.070	0.130	0.020	0.020	0.080	0.360	0.430	0.400	0.510	0.450	0.460
CHARISten	0.020	0.060	0.110	0.040	0.100	0.030	0.430	0.500	0.540	0.520	0.510	0.530
CIMIS44AirTemperature3	0.060	1.000	0.980	0.500	0.180	0.470	0.640	0.740	0.750	0.740	0.620	0.740
CIMIS44AirTemperature5	0.390	0.990	0.990	0.960	0.200	0.710	0.780	0.750	0.810	0.920	0.560	0.720
ECG2	1.000	1.000	1.000	0.620	0.900	1.000	0.830	0.740	0.840	0.630	0.780	0.600
ECG3	0.360	0.810	0.980	0.800	0.840	0.480	0.540	0.700	0.770	0.680	0.450	0.610
Fantasia	0.750	1.000	0.950	0.660	0.870	0.550	0.730	0.630	0.640	0.710	0.650	0.610
GP711MarkerLFM5z4	0.930	0.810	1.000	0.500	0.640	0.950	0.540	0.630	0.730	0.600	0.620	0.720
GP711MarkerLFM5z5	0.760	0.690	0.970	0.310	0.480	0.900	0.690	0.760	0.720	0.520	0.630	0.840
InternalBleeding4	NaN	1.000	NaN	NaN	NaN	NaN	NaN	0.650	NaN	NaN	NaN	NaN
InternalBleeding5	0.940	1.000	1.000	1.000	0.920	1.000	0.460	0.600	0.690	0.760	0.630	0.940
Italianpowerdemand	0.010	0.390	0.740	0.590	0.010	0.440	0.450	0.800	0.770	0.700	0.480	0.710
Lab2Cmac011215EPG5	0.990	0.970	0.980	0.340	0.600	0.990	0.770	0.620	0.630	0.710	0.640	0.610
Lab2Cmac011215EPG6	0.410	0.090	0.100	0.260	0.100	0.170	0.700	0.480	0.480	0.600	0.520	0.450
MesoplodonDensirostris	1.000	0.910	0.840	0.790	1.000	1.000	0.850	0.730	0.720	0.740	0.690	0.790
PowerDemand1	0.870	0.260	0.440	0.490	0.760	0.950	0.720	0.520	0.540	0.530	0.600	0.750
TkeepFirstMARS	0.010	0.080	0.150	0.020	0.020	0.230	0.520	0.570	0.760	0.460	0.500	0.790
TkeepSecondMARS	0.830	0.950	1.000	0.160	0.120	0.950	0.720	0.950	0.910	0.970	0.810	0.980
WalkingAceleration5	0.990	1.000	1.000	0.910	0.870	0.930	0.940	0.860	0.870	0.930	0.910	0.850
apneaecg	0.400	0.210	0.200	0.250	0.310	0.260	0.580	0.690	0.690	0.590	0.580	0.760
apneaecg2	0.650	0.940	1.000	1.000	1.000	0.650	0.790	0.750	0.740	0.730	0.650	0.610
gait1	0.180	0.710	0.360	0.070	0.410	0.520	0.630	0.650	0.570	0.600	0.580	0.600
gaitHunt1	0.080	0.500	0.430	0.020	0.100	0.300	0.810	0.640	0.680	0.570	0.710	0.840
insectEPG2	0.120	0.110	0.230	0.140	0.810	0.960	0.650	0.570	0.820	0.650	0.560	0.730
insectEPG4	0.980	1.000	1.000	0.460	0.210	0.850	0.690	0.700	0.720	0.730	0.490	0.650
ltstdbs30791AS	1.000	1.000	1.000	1.000	1.000	1.000	0.780	0.760	0.810	0.770	0.740	0.670
mit14046longtermecg	0.450	0.560	0.590	0.530	0.580	0.600	0.790	0.660	0.660	0.640	0.610	0.840
park3m	0.150	0.560	0.640	0.200	0.630	0.930	0.630	0.750	0.780	0.650	0.540	0.780
qtdbSel1005V	0.410	0.570	0.650	0.400	0.390	0.530	0.520	0.640	0.640	0.490	0.610	0.540
qtdbSel100MLII	0.420	0.780	0.840	0.410	0.600	0.870	0.620	0.580	0.620	0.590	0.580	0.650
resperation1	0.000	0.040	0.150	0.030	0.010	0.030	0.750	0.500	0.670	0.740	0.470	0.670
s20101mML2	0.690	0.650	0.710	0.150	0.050	0.080	0.640	0.760	0.720	0.690	0.640	0.690
sddb49	0.890	1.000	1.000	0.880	0.940	1.000	0.660	0.730	0.730	0.740	0.580	0.680
sel840mECG1	0.160	0.610	0.660	0.280	0.210	0.360	0.620	0.720	0.720	0.870	0.650	0.600
sel840mECG2	0.150	0.360	0.390	0.320	0.280	0.210	0.590	0.710	0.690	0.490	0.520	0.520
tilt12744mtable	0.070	0.110	0.240	0.100	0.000	0.030	0.480	0.670	0.740	0.660	0.510	0.640
tilt12754table	0.230	0.590	0.640	0.040	0.060	0.050	0.600	0.750	0.820	0.790	0.550	0.750
tiltAPB2	0.920	0.960	0.980	0.360	0.830	0.380	0.770	0.750	0.770	0.710	0.600	0.700
tiltAPB3	0.170	0.480	0.850	0.030	0.050	0.090	0.680	0.610	0.650	0.540	0.440	0.580
weallwalk	0.000	0.520	0.580	0.070	0.130	0.170	0.730	0.930	0.930	0.860	0.870	0.850

Table 22. Anomaly detection performance measured using adj. best F_1 and VUS-ROC for a subset of 45 datasets sampled from the UCR Anomaly archive.

report accuracy as the evaluation metric.

Hyperparameters. The hyperparameters used for evaluating classification experiments are shown in Table 25.

F.3. Anomaly Detection

Task Description. Given a time series $\mathcal{T}$, anomaly detection is a binary classification problem, where the goal is to detect whether a time step x_i is indicative of an anomaly or not. As shown in Fig. 4 (v), to detect anomalies in $\mathcal{T}$, we retain MOMENT's reconstruction head and use it to reconstruct the input time series. Then, time steps where observations and predictions differ beyond a certain threshold are classified as anomalies[15].

Datasets. We conduct experiments on a subset of 46 univariate time series from the UCR Anomaly Archive (Wu & Keogh, 2023), as enumerated in Table 11. When choosing the subset of time series, we prioritized coverage over different domains and data sources represented in the archive.

Baselines. We compare MOMENT with 2 state-of-the-art anomaly detection methods DGHL (Challu et al., 2022) and Anomaly Transformer (Xu et al., 2022) along with TimesNet and GPT4TS. We also include k-Nearest Neighbors (with $k = 5$) (Ramaswamy et al., 2000), a classical anomaly detection method in our experiments. In the zero-shot setting, we compare MOMENT to randomly initialized DGHL (DGHL_0)[16] and k-NN.

---

[15]Estimating good thresholds for anomaly detection is beyond the scope of this study and an active area of research (Goswami et al., 2023a; Schmidl et al., 2022).

[16]Randomly initialized DGHL is not a trivial zero-shot baseline, since it performs gradient descent to find the best latent z that minimizes reconstruction error during inference time (Challu et al., 2022).

Experimental Setting. All algorithms use a fixed anomaly detection window size (= 512). Based on prior work (Wu et al., 2023; Zhou et al., 2023), we use the mean squared error between predictions and observations as the anomaly criterion[17]. Following prior work (Goswami et al., 2023a), we downsample all time series longer than 2560 timesteps by a factor of 10 to speed up the training and evaluation process.

We report two anomaly detection metrics: adjusted best F_1 which is frequently used in practice (Goswami et al., 2023a; Challu et al., 2022), and the recently proposed volume under ROC surface (VUS-ROC) metric (Paparrizos et al., 2022a). For both metrics, higher scores are better.

Hyperparameters. The hyperparameters used for training all models in our anomaly detection experiments are shown in Table 26.

F.4. Imputation

Task Description. Consider a time series $\mathcal{T} = [x_1, ..., x_L]$ and an observation mask $\mathcal{M} = [m_1, ..., m_L]$, where $m_i = 0$ if x_i is missing and $m_i = 1$ if x_i is observed. Then imputation is the task of estimating the missing values $\mathcal{T}$ by exploiting its observed values. We treat a patch as observed only if all its time steps are observed. For the remaining patches, we replace their patch embeddings with [MASK] and use MOMENT's default reconstruction head to impute its values (Fig. 4 (iv)).

Datasets. We evaluate imputation performance on 6 real-world datasets from domains where missing data is a common problem: 4 subsets of Electricity Transformer Temperature (ETT), Weather, and Electricity (Wu et al., 2023; Zhou et al., 2023).

Baselines. We compare the two variants of MOMENT with 3 state-of-the-art deep learning methods, TimesNet, FPT, and DGHL; and 3 statistical interpolation methods, Cubic Spline, Linear, and 1-D Nearest Neighbor interpolation.

Experimental Setting. To evaluate the models' ability to interpolate missing values, we randomly mask contiguous sub-sequences of length 8. Instead of masking contiguous sub-sequences, previous studies (Wu et al., 2023; Zhou et al., 2023) mask individual time points, making the imputation task much easier. The results from prior studies are shown in Table 28. We observe that the statistical methods perform similarly to transformer methods, owing to the ease of the task. For our experiments involving randomly masking patches of length 8, our results are shown in Table 29. We measure the imputation performance of models using mean squared error, over 4 different masking rates: 12.5%, 25%, 37.5%, and 50%. f

Hyperparameters. The hyperparameters used for training all models in our imputation experiments are shown in Table 27.

F.5. What is MOMENT Learning?

To investigate what MOMENT is learning, we conducted a series of experiments using synthetically generated sine waves to evaluate MOMENT's ability to capture changes in trend, amplitude, frequencies, baselines, and phase of time series. In each experiment, c controls the factor of interest, for example the power of the trend polynomial $c \in (\frac{1}{8}, 8)$ (Oreshkin et al., 2020) (Fig. 9), and frequency $c \in (1, 32)$ of the generated sine waves (Fig. 9). We generate multiple sine waves by varying c, derive their sequence-level representations using MOMENT (Sec. 3.4), and visualize them in a 2- dimensional space using PCA and t-SNE (van der Maaten, 2014) in Fig. 4 and Fig. 7.

We also study the composition of the learnable mask embedding and the relationship between frequency and reconstruction error in a zero-shot setting. We find that the learned mask embedding is approximately composed of numbers drawn from the standard normal and that MOMENT can reconstruct lower frequency signals better. We observed a curious spike in reconstruction error around time series of frequency $c = 64$. (Fig. 11)

F.6. Impact of Model Size

We studied the impact of scaling the size of the model and training data on zero-shot forecasting, imputation, and anomaly detection performance. As shown in Fig. x, we found that increasing the size of the model generally improved zero-shot performance (lower MSE and sMAPE, higher VUS-ROC). Since varying the size of the pre-training dataset is expensive, we instead look at the zero-shot performance of model checkpoints before completing the first epoch. Our findings suggest that increasing the diversity in training data may also improve zero-shot performance.

(i) Trend   *(ii)* Amplitude   *(iii)* Frequency   *(iv)* Basline Shift   *(v)* Auto-correlation
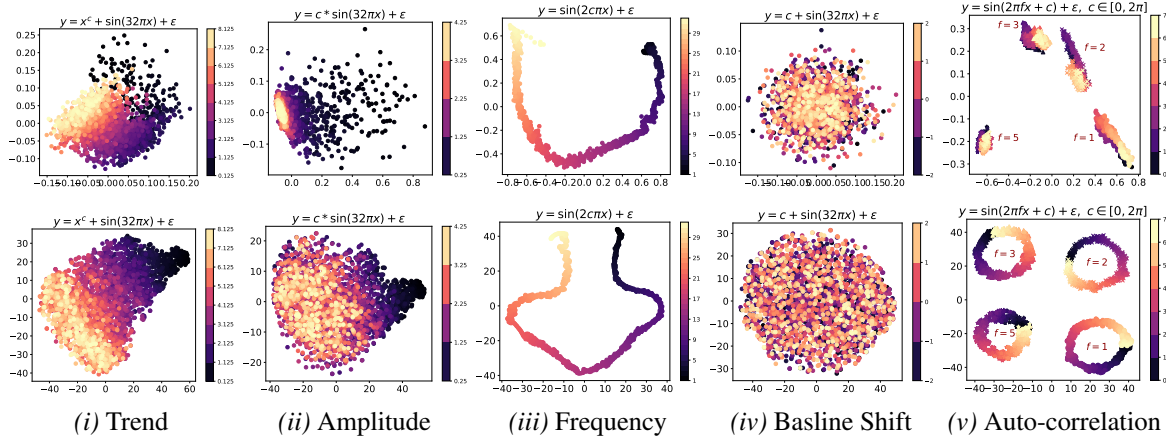
Figure 7. What is MOMENT learning? Structure in the PCA (top) and t-SNE (bottom) visualizations of the embeddings of synthetically generated sinusoids suggest that MOMENT can capture subtle trend, scale, frequency, and auto-correlation information. ϵ denotes gaussian noise with 0 mean and 0.1 standard deviation. c controls the factor of interest, i.e. the power of the trend polynomial, amplitude, and frequency of the sine waves in experiments (i), (ii) & (iii), respectively.
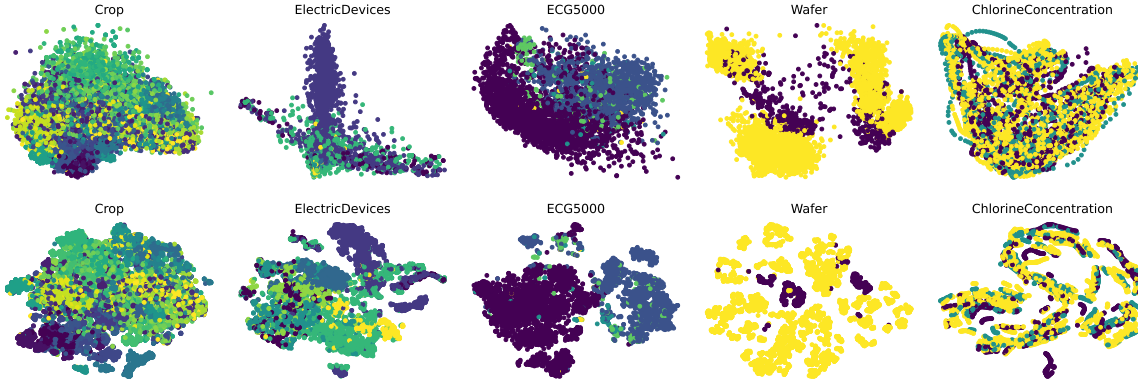
Figure 8. PCA (top) and t-SNE (bottom) visualizations of representations learned by MOMENT on the 5 largest UCR datasets. Different colors represent different classes. Even without dataset-specific fine-tuning, MOMENT learns distinct representations for different classes

F.7. Training losses

F.8. Efficiency Analysis

G. Transparency Index

H. Results Sources

I. Radar Plot

We generate a radar plot (Fig. 1) to visually compare MOMENT with GPT4TS and TimesNet. The values obtained by each method for a given task are min-max normalized with respect to the other methods for each of the 5 downstream tasks. For imputation, long- and short-horizon forecasting, we report $1-$ the normalized MSE or sMAPE for the methods on the weather and (subset of) M4 datasets, respectively. For classification and anomaly detection, we report the average accuracy and VUS-ROC of the methods across all the datasets.

---

[17]To ensure a fair comparison, we do not use Anomaly Transformer's joint criterion as the anomaly score. We believe that this might put the Anomaly Transformer at some disadvantage in our experiments.

Figure 9. Examples of sinusoids used in the interpretability experiments.

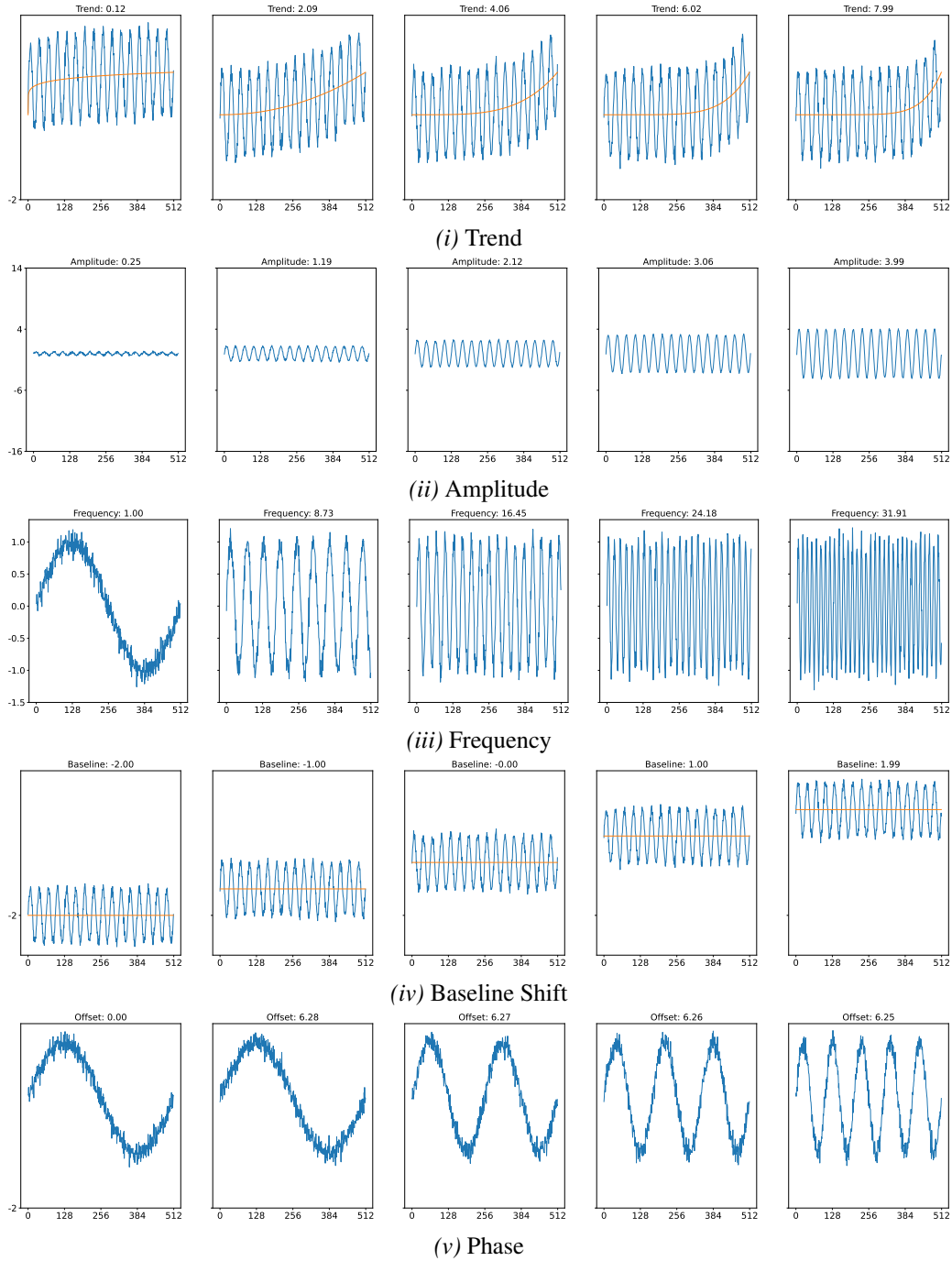| Dataset	MOMENT$_0$	TimesNet	GPT4TS	TS2Vec	T-Loss	TNC	TS-TCC	TST	CNN	Encoder	FCN	MCDNN	MLP	ResNet	t-LeNet	TWIESN	DTW
GestureMidAirD2	0.608	0.131	0.200	0.469	0.546	0.254	0.254	0.138	0.518	0.480	0.631	0.500	0.545	0.668	0.038	0.575	0.608
UWaveGestureLibraryX	0.821	0.688	0.749	0.795	0.785	0.733	0.733	0.569	0.721	0.771	0.754	0.726	0.768	0.781	0.127	0.608	0.728
GesturePebbleZ2	0.816	0.310	0.285	0.873	0.899	0.430	0.430	0.380	0.778	0.796	0.781	0.720	0.701	0.777	0.184	0.843	0.671
ECG5000	0.942	0.584	0.584	0.935	0.933	0.941	0.941	0.928	0.928	0.941	0.940	0.933	0.930	0.935	0.584	0.922	0.924
OSULeaf	0.785	0.397	0.231	0.851	0.760	0.723	0.723	0.545	0.482	0.554	0.979	0.419	0.560	0.980	0.182	0.628	0.591
MedicalImages	0.762	0.571	0.496	0.789	0.750	0.747	0.747	0.632	0.671	0.664	0.778	0.627	0.719	0.770	0.514	0.649	0.737
Ham	0.581	0.686	0.781	0.714	0.724	0.743	0.743	0.524	0.720	0.682	0.707	0.718	0.699	0.758	0.514	0.768	0.467
DistalPhalanxTW	0.612	0.604	0.619	0.698	0.676	0.676	0.676	0.568	0.671	0.694	0.695	0.685	0.610	0.663	0.285	0.591	0.590
ProximalPhalanxOutlineCorrect	0.856	0.869	0.801	0.887	0.859	0.873	0.873	0.770	0.807	0.768	0.907	0.866	0.730	0.920	0.684	0.817	0.784
FreezerRegularTrain	0.982	0.926	0.829	0.986	0.956	0.989	0.989	0.922	0.987	0.760	0.997	0.973	0.906	0.998	0.500	0.946	0.899
TwoLeadECG	0.847	0.633	0.658	0.986	0.999	0.976	0.976	0.871	0.877	0.784	0.999	0.806	0.753	1.000	0.500	0.949	0.905
GunPointMaleVersusFemale	0.991	0.601	0.475	1.000	0.997	0.997	0.997	1.000	0.977	0.978	0.997	0.952	0.980	0.992	0.525	0.988	0.997
Trace	1.000	0.760	0.710	1.000	0.990	1.000	1.000	1.000	0.952	0.740	1.000	0.902	0.806	1.000	0.240	0.934	1.000
SmoothSubspace	0.820	0.440	0.453	0.980	0.960	0.953	0.953	0.827	0.976	0.964	0.975	0.963	0.980	0.980	0.333	0.849	0.827
MiddlePhalanxTW	0.532	0.506	0.571	0.584	0.591	0.610	0.610	0.506	0.551	0.597	0.501	0.562	0.536	0.495	0.286	0.569	0.506
SyntheticControl	0.990	0.467	0.437	0.997	0.987	0.990	0.990	0.490	0.987	0.973	0.989	0.953	0.973	0.997	0.167	0.879	0.993
ShapesAll	0.815	0.238	0.237	0.902	0.848	0.773	0.773	0.733	0.617	0.679	0.894	0.599	0.776	0.926	0.017	0.643	0.768
AllGestureWiimoteX	0.607	0.209	0.237	0.777	0.763	0.697	0.697	0.259	0.411	0.475	0.713	0.261	0.477	0.741	0.100	0.522	0.716
Wafer	0.997	0.989	0.994	0.998	0.992	0.994	0.994	0.991	0.961	0.998	0.997	0.992	0.996	0.998	0.892	0.916	0.980
FaceFour	0.852	0.830	0.659	0.932	0.920	0.773	0.773	0.511	0.905	0.852	0.930	0.711	0.836	0.955	0.295	0.857	0.830
CricketX	0.749	0.523	0.531	0.782	0.713	0.731	0.731	0.385	0.535	0.644	0.794	0.513	0.591	0.799	0.074	0.627	0.754
DistalPhalanxOutlineCorrect	0.717	0.786	0.659	0.761	0.775	0.754	0.754	0.728	0.772	0.724	0.760	0.759	0.727	0.770	0.583	0.711	0.717
ChlorineConcentration	0.765	0.618	0.565	0.832	0.749	0.753	0.753	0.562	0.608	0.583	0.817	0.662	0.800	0.853	0.533	0.554	0.648
Chinatown	0.965	0.274	0.857	0.965	0.951	0.983	0.983	0.936	0.977	0.966	0.980	0.945	0.872	0.978	0.726	0.825	0.957
GestureMidAirD1	0.646	0.285	0.292	0.608	0.608	0.369	0.369	0.208	0.534	0.528	0.695	0.518	0.575	0.698	0.038	0.549	0.569
MiddlePhalanxOutlineAgeGroup	0.461	0.344	0.526	0.636	0.656	0.630	0.630	0.617	0.534	0.577	0.535	0.558	0.522	0.545	0.571	0.578	0.500
UMD	0.993	0.681	0.368	1.000	0.993	0.986	0.986	0.910	0.960	0.771	0.988	0.842	0.949	0.990	0.333	0.835	0.993
Crop	0.734	0.388	0.341	0.756	0.722	0.742	0.742	0.710	0.670	0.760	0.738	0.687	0.618	0.743	0.042	0.489	0.665
GesturePebbleZ1	0.849	0.512	0.605	0.930	0.919	0.395	0.395	0.500	0.844	0.821	0.880	0.769	0.792	0.901	0.163	0.840	0.791
WordSynonyms	0.688	0.335	0.451	0.676	0.691	0.531	0.531	0.422	0.568	0.557	0.561	0.470	0.599	0.617	0.219	0.506	0.649
ArrowHead	0.743	0.360	0.429	0.857	0.766	0.737	0.737	0.771	0.717	0.630	0.843	0.678	0.784	0.838	0.303	0.689	0.703
Wine	0.537	0.519	0.611	0.870	0.815	0.778	0.778	0.500	0.519	0.556	0.611	0.500	0.541	0.722	0.500	0.744	0.574
Coffee	0.893	0.964	0.679	1.000	1.000	1.000	1.000	0.821	1.000	0.886	1.000	0.979	0.993	1.000	0.507	0.979	1.000
Earthquakes	0.748	0.741	0.748	0.748	0.748	0.748	0.748	0.748	0.709	0.740	0.725	0.748	0.727	0.712	0.748	0.748	0.719
Herring	0.594	0.531	0.578	0.641	0.594	0.594	0.594	0.594	0.531	0.512	0.644	0.572	0.491	0.600	0.594	0.625	0.531
Beef	0.833	0.400	0.167	0.767	0.667	0.600	0.600	0.500	0.767	0.707	0.680	0.507	0.713	0.753	0.200	0.527	0.633
MiddlePhalanxOutlineCorrect	0.467	0.512	0.519	0.838	0.825	0.818	0.818	0.753	0.744	0.752	0.795	0.796	0.755	0.826	0.570	0.743	0.698
ECGFiveDays	0.804	0.519	0.561	1.000	1.000	0.878	0.878	0.763	0.874	0.842	0.985	0.800	0.973	0.966	0.497	0.723	0.768
Yoga	0.834	0.672	0.691	0.887	0.837	0.791	0.791	0.830	0.786	0.753	0.837	0.741	0.856	0.867	0.536	0.626	0.837
Adiac	0.688	0.565	0.598	0.762	0.675	0.767	0.767	0.550	0.393	0.318	0.841	0.620	0.391	0.833	0.023	0.428	0.604
MoteStrain	0.774	0.700	0.681	0.861	0.851	0.843	0.843	0.768	0.885	0.872	0.936	0.691	0.855	0.924	0.539	0.809	0.835
Strawberry	0.951	0.946	0.935	0.962	0.954	0.965	0.965	0.916	0.952	0.959	0.975	0.958	0.959	0.980	0.643	0.911	0.941
InsectWingbeatSound	0.607	0.529	0.598	0.630	0.597	0.415	0.415	0.266	0.585	0.630	0.392	0.587	0.604	0.499	0.091	0.435	0.355
DodgerLoopWeekend	0.826	0.638	0.804	0.964	NaN	NaN	NaN	0.732	0.974	0.983	0.904	0.978	0.978	0.952	0.739	0.954	0.949
Meat	0.917	0.433	0.667	0.950	0.950	0.883	0.883	0.900	0.913	0.787	0.803	0.787	0.893	0.990	0.333	0.970	0.933
MelbournePedestrian	0.876	0.718	0.207	0.959	0.944	0.949	0.949	0.741	0.813	0.884	0.912	0.840	0.863	0.909	0.100	0.730	0.791
FaceAll	0.791	0.177	0.147	0.771	0.786	0.813	0.813	0.504	0.774	0.794	0.938	0.720	0.794	0.867	0.080	0.673	0.808
FacesUCR	0.811	0.679	0.462	0.924	0.884	0.863	0.863	0.543	0.873	0.867	0.943	0.775	0.831	0.954	0.143	0.641	0.905
AllGestureWiimoteY	0.666	0.223	0.160	0.793	0.726	0.741	0.741	0.423	0.479	0.509	0.784	0.420	0.571	0.794	0.100	0.600	0.729
ShakeGestureWiimoteZ	0.960	0.020	0.080	0.940	0.920	0.860	0.860	0.760	0.580	0.756	0.884	0.516	0.548	0.880	0.100	0.864	0.860
BME	0.960	0.467	0.367	0.993	0.993	0.933	0.933	0.760	0.947	0.827	0.836	0.896	0.905	0.999	0.333	0.819	0.900
FordB	0.798	0.754	0.677	0.794	0.793	0.815	0.815	0.507	0.749	0.777	0.772	0.698	0.707	0.813	0.503	0.512	0.620
Fish	0.800	0.726	0.731	0.926	0.891	0.817	0.817	0.720	0.855	0.734	0.961	0.720	0.848	0.981	0.126	0.878	0.823
SonyAIBORobotSurface2	0.829	0.646	0.650	0.871	0.889	0.907	0.907	0.745	0.831	0.844	0.980	0.804	0.831	0.975	0.617	0.635	0.831
FiftyWords	0.802	0.499	0.492	0.771	0.732	0.653	0.653	0.525	0.624	0.658	0.646	0.611	0.708	0.740	0.125	0.518	0.690
ToeSegmentation1	0.925	0.456	0.561	0.917	0.939	0.930	0.930	0.807	0.598	0.706	0.961	0.559	0.589	0.957	0.526	0.882	0.772
FreezerSmallTrain	0.902	0.704	0.500	0.870	0.933	0.979	0.979	0.920	0.739	0.676	0.683	0.688	0.686	0.832	0.500	0.917	0.753
TwoPatterns	0.994	0.989	0.923	1.000	0.999	0.999	0.999	0.466	0.991	1.000	0.870	0.976	0.948	1.000	0.259	0.875	1.000
ShapeletSim	0.961	0.500	0.489	1.000	0.672	0.683	0.683	0.489	0.497	0.510	0.706	0.498	0.513	0.782	0.500	0.546	0.650
Plane	0.990	0.981	0.924	1.000	0.990	1.000	1.000	0.933	0.962	0.964	1.000	0.952	0.977	1.000	0.143	1.000	1.000
GestureMidAirD3	0.369	0.085	0.162	0.292	0.285	0.177	0.177	0.154	0.317	0.368	0.326	0.278	0.382	0.340	0.038	0.275	0.323
DiatomSizeReduction	0.879	0.967	0.987	0.984	0.984	0.977	0.977	0.961	0.954	0.880	0.346	0.646	0.909	0.301	0.301	0.914	0.967
CricketZ	0.731	0.459	0.397	0.792	0.708	0.713	0.713	0.403	0.501	0.651	0.810	0.484	0.629	0.809	0.062	0.643	0.754
Lightning7	0.726	0.575	0.562	0.863	0.795	0.685	0.685	0.411	0.647	0.696	0.825	0.559	0.616	0.827	0.260	0.608	0.726
UWaveGestureLibraryY	0.738	0.547	0.648	0.719	0.710	0.641	0.641	0.348	0.626	0.676	0.642	0.639	0.699	0.666	0.121	0.497	0.634
GunPointAgeSpan	0.962	0.494	0.494	0.987	0.994	0.994	0.994	0.991	0.912	0.890	0.996	0.887	0.934	0.997	0.494	0.965	0.918
DistalPhalanxOutlineAgeGroup	0.669	0.597	0.489	0.727	0.727	0.755	0.755	0.741	0.758	0.761	0.718	0.729	0.647	0.718	0.433	0.705	0.770
SwedishLeaf	0.923	0.894	0.899	0.941	0.914	0.923	0.923	0.738	0.884	0.902	0.967	0.841	0.845	0.963	0.064	0.837	0.792
CBF	0.960	0.761	0.830	1.000	0.983	0.998	0.998	0.898	0.959	0.977	0.994	0.908	0.869	0.996	0.332	0.896	0.997
BeetleFly	0.900	0.400	0.700	0.900	0.800	0.800	0.800	1.000	0.900	0.620	0.910	0.630	0.880	0.850	0.500	0.790	0.700
AllGestureWiimoteZ	0.537	0.221	0.116	0.746	0.723	0.689	0.689	0.447	0.375	0.396	0.692	0.287	0.439	0.726	0.100	0.516	0.643
DodgerLoopDay	0.438	0.237	0.200	0.562	NaN	NaN	NaN	0.200	0.312	0.487	0.143	0.305	0.160	0.150	0.160	0.593	0.500
GunPointOldVersusYoung	0.981	0.508	0.524	1.000	1.000	1.000	1.000	1.000	0.922	0.923	0.989	0.926	0.941	0.989	0.524	0.975	0.838
FordA	0.936	0.913	0.914	0.936	0.928	0.930	0.930	0.568	0.896	0.928	0.914	0.863	0.816	0.937	0.510	0.555	0.555
ItalyPowerDemand	0.911	0.837	0.880	0.925	0.954	0.955	0.955	0.845	0.954	0.964	0.963	0.966	0.953	0.962	0.499	0.871	0.950
ProximalPhalanxOutlineAgeGroup	0.863	0.868	0.839	0.834	0.844	0.839	0.839	0.854	0.812	0.872	0.825	0.839	0.849	0.847	0.488	0.839	0.805
GunPoint	0.927	0.887	0.847	0.980	0.980	0.993	0.993	0.827	0.948	0.784	1.000	0.907	0.928	0.991	0.493	0.989	0.907
ProximalPhalanxTW	0.712	0.800	0.712	0.824	0.771	0.800	0.800	0.780	0.777	0.791	0.761	0.775	0.767	0.773	0.341	0.784	0.761
PickupGestureWiimoteZ	0.620	0.100	0.080	0.820	0.740	0.600	0.600	0.240	0.608	0.496	0.744	0.412	0.604	0.704	0.100	0.616	0.660
SonyAIBORobotSurface1	0.729	0.542	0.589	0.903	0.902	0.899	0.899	0.724	0.690	0.729	0.958	0.655	0.692	0.961	0.429	0.725	0.725
PowerCons	0.894	0.956	0.989	0.961	0.900	0.961	0.961	0.911	0.960	0.971	0.863	0.929	0.977	0.879	0.500	0.852	0.878
PhalangesOutlinesCorrect	0.652	0.614	0.663	0.809	0.784	0.804	0.804	0.773	0.799	0.745	0.818	0.795	0.756	0.845	0.613	0.656	0.728
BirdChicken	0.850	0.450	0.550	0.800	0.850	0.650	0.650	0.650	0.710	0.510	0.940	0.540	0.740	0.880	0.500	0.620	0.750
ToeSegmentation2	0.915	0.731	0.731	0.892	0.900	0.877	0.877	0.615	0.752	0.702	0.889	0.649	0.745	0.894	0.815	0.794	0.838
CricketY	0.746	0.531	0.521	0.749	0.728	0.718	0.718	0.467	0.582	0.639	0.793	0.521	0.598	0.810	0.085	0.652	0.744
ElectricDevices	0.646	0.552	0.506	0.721	0.707	0.686	0.686	0.676	0.686	0.702	0.706	0.653	0.593	0.728	0.242	0.605	0.602
DodgerLoopGame	0.623	0.471	0.717	0.841	NaN	NaN	NaN	0.696	0.816	0.810	0.768	0.877	0.865	0.710	0.478	0.716	0.877
Fungi	0.898	0.043	0.054	0.957	1.000	0.753	0.753	0.366	0.961	0.934	0.018	0.051	0.863	0.177	0.063	0.439	0.839
Symbols	0.936	0.864	0.694	0.976	0.963	0.916	0.916	0.786	0.808	0.754	0.955	0.644	0.836	0.893	0.174	0.798	0.950
UWaveGestureLibraryZ	0.765	0.632	0.643	0.770	0.757	0.690	0.690	0.655	0.630	0.684	0.727	0.645	0.697	0.749	0.121	0.573	0.658
ECG200	0.760	0.830	0.790	0.920	0.940	0.880	0.880	0.830	0.816	0.884	0.888	0.838	0.914	0.874	0.640	0.874	0.770

Table 23. Classification accuracy of methods across 91 UCR datasets. MOMENT without fine-tuning on individual datasets demonstrates promising accuracy.

Dataset	MOMENT$_0$	TS2Vec	T-Loss	TNC	TS-TCC	TST	DTW
ArticularyWordRecognition	0.990	0.987	0.943	0.973	0.953	0.977	0.987
AtrialFibrillation	0.200	0.200	0.133	0.133	0.267	0.067	0.200
BasicMotions	1.000	0.975	1.000	0.975	1.000	0.975	0.975
Cricket	0.986	0.972	0.972	0.958	0.917	1.000	1.000
DuckDuckGeese	0.600	0.680	0.650	0.460	0.380	0.620	0.600
EigenWorms	0.809	0.847	0.840	0.840	0.779	0.748	0.618
Epilepsy	0.993	0.964	0.971	0.957	0.957	0.949	0.964
ERing	0.959	0.874	0.133	0.852	0.904	0.874	0.133
EthanolConcentration	0.357	0.308	0.205	0.297	0.285	0.262	0.323
FaceDetection	0.633	0.501	0.513	0.536	0.544	0.534	0.529
FingerMovements	0.490	0.480	0.580	0.470	0.460	0.560	0.530
HandMovementDirection	0.324	0.338	0.351	0.324	0.243	0.243	0.231
Handwriting	0.308	0.515	0.451	0.249	0.498	0.225	0.286
Heartbeat	0.722	0.683	0.741	0.746	0.751	0.746	0.717
JapaneseVowels	0.716	0.984	0.989	0.978	0.930	0.978	0.949
Libras	0.850	0.867	0.883	0.817	0.822	0.656	0.870
LSST	0.411	0.537	0.509	0.595	0.474	0.408	0.551
MotorImagery	0.500	0.510	0.580	0.500	0.610	0.500	0.500
NATOPS	0.828	0.928	0.917	0.911	0.822	0.850	0.883
PEMS-SF	0.896	0.682	0.676	0.699	0.734	0.740	0.711
PenDigits	0.972	0.989	0.981	0.979	0.974	0.560	0.977
PhonemeSpectra	0.233	0.233	0.222	0.207	0.252	0.085	0.151
RacketSports	0.796	0.855	0.855	0.776	0.816	0.809	0.803
SelfRegulationSCP1	0.840	0.812	0.843	0.799	0.823	0.754	0.775
SelfRegulationSCP2	0.478	0.578	0.539	0.550	0.533	0.550	0.539
SpokenArabicDigits	0.981	0.988	0.905	0.934	0.970	0.923	0.963
StandWalkJump	0.400	0.467	0.333	0.400	0.333	0.267	0.200
UWaveGestureLibrary	0.909	0.906	0.875	0.759	0.753	0.575	0.903
InsectWingbeat	0.246	0.466	0.156	0.469	0.264	0.105	NaN
Mean	0.670	0.694	0.646	0.660	0.657	0.605	0.638
Median	0.722	0.683	0.676	0.746	0.751	0.620	0.664
Std.	0.274	0.255	0.296	0.267	0.263	0.294	0.296
Mean Rank	3.466	2.862	3.603	4.362	4.121	5.069	4.429
Median Rank	3.0	2.5	4.0	5.0	5.0	5.5	4.5
Wins/Losses	101.5/71.5	119.0/54.0	97.5/75.5	75.5/97.5	82.5/90.5	55.0/118.0	72.0/96.0

Table 24. Classification accuracy of methods across 29 UEA datasets. MOMENT without fine-tuning on individual datasets demonstrates promising accuracy.

Model	Hyper-parameters		
MOMENT$_0$	sequence length:	512	
	patch length:	8	
	patch stride length:	8	
SVM	C:	$\{0.0001, 0.001, 0.01, 0.1, 1, 10, 100, 1000, 10000\}$	
	kernel:	RBF	
	degree:	3	
	cache size:	200	
	max iterations:	10000000	
	decision function shape:	One versus rest	

Table 25. Hyper-parameter values for classification.

Model	Hyper-parameters	
MOMENT_0	sequence length:	512
	patch length:	8
	patch stride length:	8
MOMENT_{LP}	sequence length:	512
	patch length:	8
	patch stride length:	8
	initial lr:	$5e-5$
Anomaly Transformer	sequence length:	512
	number of channels:	1
	k:	3
	anomaly ratio:	4.00
	model dimensions:	512
	number of heads:	8
	embedding layers:	3
	dimension of feedforward layer:	512
DGHL	sequence length:	512
	number of channels:	1
	hidden multiplier:	32
	max filters:	256
	kernel multiplier:	1
	sub-windows:	4
	size of latent z vector:	50
	number of iteration in the Langevyn dynamics inference formula:	100
	z step size:	0.1
	noise std:	0.001
GPT4TS	sequence length:	512
	gpt layers:	3
	patch length:	1
	patch stride length:	1
	transformer backbone:	GPT-2
TimesNet	sequence length:	512
	dimension of model:	16
	dimension of feedforward layer:	16
	top k:	3
	number of kernels:	6
$k-\text{NN}$	k:	5

Table 26. Hyperparameter values for anomaly detection.

Model	Hyper-parameters	
MOMENT_0	sequence length:	512
	patch length:	8
	patch stride length:	8
MOMENT_{LP}	sequence length:	512
	patch length:	8
	patch stride length:	8
	initial lr:	0.0001
GPT4TS	sequence length:	512
	gpt layers:	3
	patch length:	1
	patch stride length:	1
	transformer backbone:	GPT-2
	dimension of feedforward layer:	16
TimesNet	sequence length:	512
	dimension of model:	64
	dimension of feedforward layer:	64
	top k:	3
	number of kernels:	6

Table 27. Hyperparameter values for imputation.

33

Methods		GPT4TS		TimesNet		PatchTST		ETSformer		LightTS		DLinear		FEDformer		Stationary		Autoformer		Informer		Reformer		Naive		Linear		Nearest		Cubic	
Dataset	Mask Ratio	MSE	MAE	MSE	MAE	MSE	MAE	MSE	MAE	MSE	MAE	MSE	MAE	MSE	MAE	MSE	MAE	MSE	MAE	MSE	MAE	MSE	MAE	MSE	MAE	MSE	MAE	MSE	MAE	MSE	MAE
ETTm1	12.5%	**0.017**	**0.085**	0.023	0.101	0.041	0.130	0.096	0.229	0.093	0.206	0.080	0.193	0.052	0.166	0.032	0.119	0.046	0.144	0.063	0.180	0.042	0.146	0.034	0.109	0.033	0.112	0.055	0.142	0.052	0.135
	25%	**0.022**	**0.096**	0.023	0.101	0.044	0.135	0.096	0.229	0.093	0.206	0.080	0.193	0.052	0.166	0.032	0.119	0.046	0.144	0.063	0.180	0.042	0.146	0.066	0.153	0.036	0.112	0.056	0.142	0.060	0.142
	37.5%	**0.029**	**0.111**	0.029	0.111	0.049	0.143	0.133	0.271	0.113	0.231	0.103	0.219	0.069	0.191	0.039	0.131	0.057	0.161	0.079	0.200	0.063	0.182	0.077	0.164	0.038	0.117	0.060	0.146	0.071	0.151
	50%	0.040	0.128	**0.036**	**0.124**	0.055	0.151	0.186	0.323	0.134	0.255	0.132	0.248	0.089	0.218	0.047	0.145	0.067	0.174	0.093	0.218	0.082	0.208	0.094	0.178	0.042	0.123	0.066	0.153	0.100	0.164
	Avg	0.028	0.105	**0.027**	0.107	0.047	0.140	0.120	0.253	0.104	0.218	0.093	0.206	0.062	0.177	0.036	0.126	0.051	0.150	0.071	0.188	0.055	0.166	0.074	0.160	0.038	0.115	0.059	0.145	0.071	0.148
ETTm2	12.5%	**0.017**	**0.076**	0.018	0.080	0.026	0.094	0.108	0.239	0.034	0.127	0.056	0.159	0.056	0.159	0.021	0.088	0.023	0.092	0.133	0.270	0.108	0.228	0.038	0.095	0.023	0.077	0.035	0.091	0.033	0.097
	25%	**0.020**	**0.080**	0.020	0.085	0.028	0.099	0.164	0.294	0.042	0.143	0.085	0.196	0.080	0.195	0.024	0.096	0.026	0.101	0.135	0.272	0.136	0.262	0.041	0.100	0.025	0.081	0.036	0.093	0.039	0.103
	37.5%	**0.022**	**0.087**	0.023	0.091	0.030	0.104	0.237	0.356	0.051	0.159	0.106	0.222	0.110	0.231	0.027	0.103	0.030	0.108	0.155	0.293	0.175	0.300	0.044	0.085	0.027	0.085	0.038	0.095	0.047	0.111
	50%	**0.025**	**0.095**	0.026	0.098	0.034	0.110	0.323	0.421	0.059	0.174	0.131	0.247	0.156	0.276	0.030	0.108	0.035	0.119	0.200	0.333	0.211	0.329	0.051	0.115	0.030	0.090	0.041	0.100	0.062	0.122
	Avg	**0.021**	**0.084**	0.022	0.088	0.029	0.102	0.208	0.327	0.046	0.151	0.101	0.215	0.101	0.215	0.026	0.099	0.029	0.105	0.156	0.292	0.157	0.280	0.044	0.099	0.026	0.083	0.038	0.095	0.045	0.109
ETTh1	12.5%	**0.043**	**0.140**	0.057	0.159	0.093	0.201	0.126	0.263	0.240	0.345	0.151	0.267	0.070	0.190	0.060	0.165	0.074	0.182	0.114	0.234	0.074	0.194	0.211	0.275	0.083	0.183	0.181	0.260	0.107	0.207
	25%	**0.054**	**0.156**	0.069	0.178	0.107	0.217	0.169	0.304	0.265	0.364	0.180	0.292	0.106	0.236	0.080	0.189	0.090	0.203	0.140	0.262	0.102	0.227	0.259	0.298	0.098	0.197	0.192	0.266	0.127	0.224
	37.5%	**0.072**	**0.180**	0.084	0.196	0.120	0.230	0.220	0.347	0.296	0.382	0.215	0.318	0.124	0.258	0.102	0.212	0.109	0.222	0.174	0.293	0.135	0.261	0.323	0.326	0.119	0.215	0.215	0.277	0.160	0.245
	50%	0.107	0.216	**0.102**	**0.215**	0.141	0.248	0.293	0.402	0.334	0.404	0.257	0.347	0.165	0.299	0.133	0.240	0.137	0.248	0.215	0.325	0.179	0.298	0.423	0.366	0.158	0.242	0.257	0.297	0.235	0.279
	Avg	**0.069**	**0.173**	0.078	0.187	0.115	0.224	0.202	0.329	0.284	0.373	0.201	0.306	0.117	0.246	0.094	0.201	0.103	0.214	0.161	0.279	0.122	0.245	0.304	0.317	0.114	0.209	0.211	0.275	0.157	0.239
ETTh2	12.5%	**0.039**	**0.125**	0.040	0.130	0.057	0.152	0.187	0.319	0.101	0.231	0.100	0.216	0.095	0.212	0.042	0.133	0.044	0.138	0.305	0.431	0.163	0.289	0.090	0.167	0.058	0.134	0.085	0.162	0.091	0.172
	25%	**0.044**	**0.135**	0.046	0.141	0.061	0.158	0.279	0.390	0.115	0.246	0.127	0.247	0.137	0.258	0.049	0.147	0.050	0.149	0.322	0.444	0.206	0.331	0.097	0.176	0.060	0.138	0.088	0.165	0.101	0.179
	37.5%	**0.051**	**0.147**	0.052	0.151	0.067	0.166	0.400	0.465	0.126	0.257	0.158	0.276	0.187	0.304	0.056	0.158	0.060	0.163	0.353	0.462	0.252	0.370	0.105	0.185	0.064	0.144	0.091	0.169	0.118	0.190
	50%	**0.059**	**0.158**	0.060	0.162	0.073	0.174	0.602	0.572	0.136	0.268	0.183	0.299	0.232	0.341	0.065	0.170	0.068	0.173	0.369	0.472	0.316	0.419	0.118	0.199	0.071	0.153	0.097	0.176	0.150	0.205
	Avg	**0.048**	**0.141**	0.049	0.146	0.065	0.163	0.367	0.436	0.119	0.250	0.142	0.259	0.163	0.279	0.053	0.152	0.055	0.156	0.337	0.452	0.234	0.352	0.102	0.182	0.063	0.142	0.090	0.168	0.115	0.186
ECL	12.5%	0.080	0.194	0.085	0.202	0.055	0.160	0.196	0.321	0.102	0.229	0.092	0.214	0.107	0.237	0.093	0.210	0.089	0.210	0.218	0.326	0.190	0.308	0.214	0.293	0.079	0.182	0.181	0.271	0.091	0.196
	25%	0.087	0.203	0.089	0.206	0.065	0.175	0.207	0.332	0.121	0.252	0.118	0.247	0.120	0.251	0.097	0.214	0.096	0.220	0.219	0.326	0.197	0.312	0.266	0.324	0.094	0.199	0.194	0.280	0.115	0.217
	37.5%	0.094	0.211	0.094	0.213	0.076	0.189	0.219	0.344	0.141	0.273	0.144	0.276	0.136	0.266	0.102	0.220	0.104	0.229	0.222	0.328	0.203	0.315	0.339	0.366	0.117	0.223	0.220	0.296	0.152	0.245
	50%	0.101	0.220	0.100	0.221	0.091	0.208	0.235	0.357	0.160	0.293	0.175	0.305	0.158	0.284	0.108	0.228	0.113	0.239	0.228	0.331	0.210	0.319	0.447	0.424	0.156	0.259	0.264	0.324	0.222	0.286
	Avg	0.090	0.207	0.092	0.210	0.072	0.183	0.214	0.339	0.131	0.262	0.132	0.260	0.130	0.259	0.100	0.218	0.101	0.225	0.222	0.328	0.200	0.313	0.316	0.352	0.112	0.216	0.215	0.293	0.145	0.236
Weather	12.5%	0.026	0.049	**0.025**	**0.045**	0.029	0.049	0.057	0.141	0.047	0.101	0.039	0.084	0.041	0.107	0.027	0.051	0.026	0.047	0.037	0.093	0.031	0.076	0.041	0.042	0.026	0.031	0.038	0.041	0.038	0.036
	25%	0.028	0.052	**0.029**	**0.052**	0.031	0.053	0.065	0.155	0.052	0.111	0.048	0.103	0.064	0.163	0.029	0.056	0.030	0.054	0.042	0.100	0.035	0.082	0.045	0.045	0.027	0.032	0.040	0.041	0.039	0.039
	37.5%	0.033	0.060	**0.031**	**0.057**	0.035	0.058	0.081	0.180	0.058	0.121	0.057	0.117	0.107	0.229	0.033	0.062	0.032	0.060	0.049	0.111	0.040	0.091	0.048	0.049	0.030	0.034	0.042	0.043	0.055	0.043
	50%	0.037	0.065	**0.034**	**0.062**	0.038	0.063	0.102	0.207	0.065	0.133	0.066	0.134	0.183	0.312	0.037	0.068	0.037	0.067	0.053	0.114	0.046	0.099	0.054	0.054	0.033	0.037	0.044	0.045	0.069	0.048
	Avg	0.031	0.056	**0.030**	**0.054**	0.033	0.058	0.076	0.171	0.055	0.117	0.052	0.110	0.099	0.203	0.032	0.059	0.031	0.057	0.045	0.104	0.038	0.087	0.047	0.048	0.029	0.034	0.041	0.043	0.051	0.042

Table 28. Results for the imputation task in the time-steps missing at random setting. Results averaged across 4 different masking rates: {12.5%, 25%, 37.5%, 50%}. Statistical interpolation methods such as forward and backward fill (naive), linear, nearest, and cubic interpolation perform better than many transformer-based baselines. Therefore, we consider the much harder, patches missing at random setting in our experiments.

Dataset	Mask Ratio	$MOMENT_O$		$MOMENT_{LP}$		GPT4TS		TimesNet		Naive		Linear		Nearest		Cubic	
		MSE	MAE	MSE	MAE	MSE	MAE	MSE	MAE	MSE	MAE	MSE	MAE	MSE	MAE	MSE	MAE
Weather	0.125	0.085	0.131	0.033	0.073	0.036	0.076	0.035	0.096	0.105	0.089	0.050	0.055	0.069	0.067	0.373	0.115
	0.250	0.079	0.130	0.036	0.078	0.030	0.071	0.037	0.100	0.127	0.104	0.075	0.065	0.094	0.076	0.297	0.125
	0.375	0.081	0.128	0.034	0.075	0.030	0.070	0.035	0.099	0.120	0.111	0.066	0.069	0.082	0.080	0.904	0.176
	0.500	0.081	0.129	0.035	0.075	0.026	0.069	0.035	0.098	0.124	0.127	0.066	0.078	0.086	0.090	0.831	0.197
	Mean	0.082	0.130	0.035	0.075	0.031	0.071	0.036	0.098	0.119	0.108	0.065	0.067	0.083	0.078	0.601	0.153
ETTh1	0.125	0.430	0.417	0.160	0.239	0.183	0.242	0.158	0.254	1.008	0.602	0.583	0.466	0.712	0.523	0.985	0.661
	0.250	0.373	0.392	0.142	0.238	0.278	0.267	0.154	0.261	1.311	0.686	0.833	0.540	0.954	0.581	1.433	0.772
	0.375	0.398	0.398	0.121	0.228	0.232	0.263	0.195	0.274	1.317	0.703	0.843	0.572	0.973	0.613	2.615	1.028
	0.500	0.408	0.403	0.132	0.231	0.213	0.243	0.192	0.267	1.103	0.643	0.840	0.559	0.963	0.601	3.681	1.204
	Mean	0.402	0.403	0.139	0.234	0.227	0.254	0.175	0.264	1.185	0.658	0.775	0.534	0.900	0.579	2.178	0.916
ETTh2	0.125	0.122	0.235	0.051	0.150	0.115	0.215	0.163	0.277	0.196	0.285	0.105	0.208	0.134	0.225	0.452	0.404
	0.250	0.127	0.237	0.079	0.177	0.114	0.216	0.161	0.280	0.210	0.291	0.120	0.220	0.154	0.240	0.831	0.524
	0.375	0.124	0.237	0.056	0.155	0.110	0.216	0.170	0.291	0.229	0.310	0.142	0.243	0.175	0.262	1.571	0.672
	0.500	0.127	0.242	0.056	0.154	0.098	0.207	0.186	0.295	0.265	0.329	0.171	0.264	0.199	0.279	4.823	0.966
	Mean	0.125	0.238	0.061	0.159	0.109	0.213	0.170	0.286	0.225	0.304	0.135	0.234	0.166	0.252	1.920	0.641
ETTm1	0.125	0.179	0.278	0.069	0.170	0.078	0.147	0.089	0.200	0.273	0.293	0.094	0.183	0.147	0.217	0.334	0.345
	0.250	0.206	0.290	0.071	0.169	0.071	0.144	0.080	0.194	0.395	0.341	0.114	0.202	0.171	0.234	0.539	0.424
	0.375	0.209	0.289	0.069	0.163	0.076	0.146	0.091	0.199	0.475	0.378	0.188	0.242	0.257	0.274	0.842	0.528
	0.500	0.215	0.294	0.086	0.169	0.081	0.149	0.088	0.197	0.679	0.448	0.265	0.291	0.346	0.316	1.715	0.680
	Mean	0.202	0.288	0.074	0.168	0.076	0.146	0.087	0.198	0.455	0.365	0.165	0.229	0.230	0.260	0.858	0.494
ETTm2	0.125	0.076	0.183	0.032	0.108	0.043	0.126	0.128	0.233	0.087	0.164	0.049	0.117	0.062	0.132	0.237	0.262
	0.250	0.084	0.187	0.029	0.105	0.046	0.129	0.101	0.207	0.104	0.182	0.057	0.132	0.073	0.146	0.373	0.309
	0.375	0.076	0.181	0.032	0.109	0.059	0.137	0.116	0.225	0.115	0.196	0.063	0.141	0.078	0.154	0.626	0.376
	0.500	0.077	0.183	0.031	0.110	0.059	0.140	0.103	0.212	0.144	0.222	0.080	0.162	0.102	0.177	0.899	0.477
	Mean	0.078	0.184	0.031	0.108	0.052	0.133	0.112	0.220	0.113	0.191	0.062	0.138	0.079	0.152	0.534	0.356
Electricity	0.125	0.251	0.370	0.095	0.211	0.069	0.180	0.126	0.248	1.350	0.818	0.458	0.466	0.608	0.492	0.924	0.610
	0.250	0.249	0.372	0.093	0.211	0.073	0.184	0.121	0.246	1.447	0.857	0.654	0.554	0.815	0.582	1.619	0.769
	0.375	0.250	0.371	0.094	0.211	0.071	0.181	0.125	0.248	1.518	0.888	0.836	0.637	1.031	0.675	2.507	0.959
	0.500	0.250	0.371	0.092	0.210	0.075	0.185	0.126	0.249	1.581	0.915	1.002	0.712	1.239	0.766	3.978	1.213
	Mean	0.250	0.371	0.094	0.211	0.072	0.183	0.124	0.248	1.474	0.869	0.737	0.592	0.923	0.629	2.257	0.888

Table 29. **Imputation Results.** MOMENT achieves state-of-the-art imputation results in both zero-shot and linear probe fine-tuning settings.
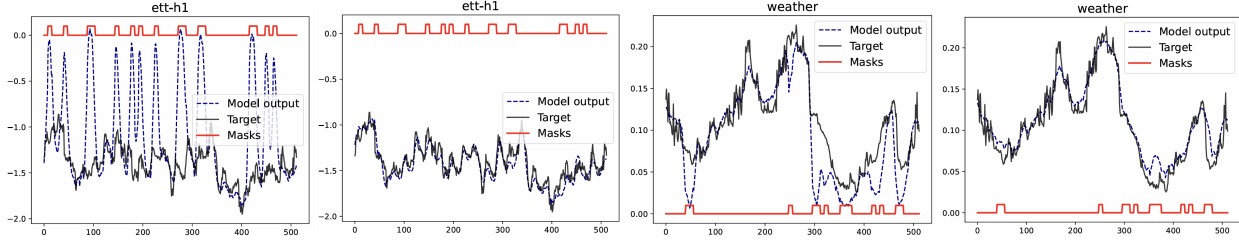
Figure 10. Masking using a `[MASK]` tokens allows `MOMENT` to reconstruct time series in a zero-shot setting. Since zeros contain information, they bias model predictions. For two datasets ETTh1 and Weather, we mask the time series with zeros on the left and special mask tokens on the right.
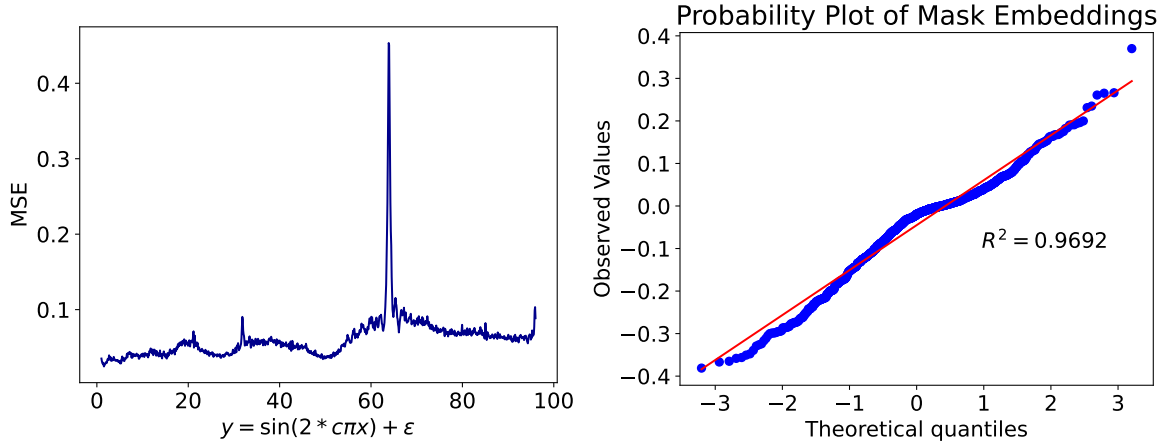

Figure 11. (*Left*) `MOMENT` can reconstruct lower frequency time series better in a zero-shot setting. (*Right*) The learned mask token is approximately composed of numbers drawn from a standard normal.

Dataset	Pred_horizon	MOMENT$_{small}$		MOMENT$_{base}$		MOMENT$_{large}$	
		MSE	MAE	MSE	MAE	MSE	MAE
Weather	96	0.167	0.224	0.156	0.211	0.151	0.207
	192	0.210	0.259	0.198	0.248	0.195	0.246
	336	0.256	0.292	0.247	0.284	0.245	0.285
	720	0.315	0.334	0.315	0.334	0.316	0.333
ETTh1	96	0.388	0.411	0.391	0.414	0.381	0.406
	192	0.420	0.432	0.420	0.433	0.412	0.425
	336	0.443	0.451	0.424	0.438	0.429	0.442
	720	0.457	0.473	0.426	0.451	0.453	0.468

Table 30. Long-horizon forecasting scaling experiments for MOMENT$_{small}$, MOMENT$_{base}$, and MOMENT$_{large}$.

Metric		MOMENT$_{small}$	MOMENT$_{base}$	MOMENT$_{large}$
Adj. F1	Mean	0.480	0.572	0.569
	Median	0.450	0.641	0.607
	Std.	0.378	0.383	0.372
Vus ROC	Mean	0.643	0.677	0.660
	Median	0.644	0.669	0.657
	Std.	0.137	0.121	0.130

Table 31. Zero-shot anomaly detection scaling experiments for MOMENT$_{small}$, MOMENT$_{base}$, and MOMENT$_{large}$.

	MOMENT$_{\texttt{small}}$	MOMENT$_{\texttt{base}}$	MOMENT$_{\texttt{large}}$
Mean	0.716705	0.766437	0.763933
Median	0.720930	0.771078	0.766667
Std.	0.155945	0.156763	0.160345
Avg. rank	2.686813	1.659341	1.653846
Median rank	3.000000	2.000000	1.50
Wins/Losses	28.5/153.5	122.0/60.0	122.5/59.5

Table 32. Zero-shot classification scaling experiments for MOMENT$_{\texttt{small}}$, MOMENT$_{\texttt{base}}$, and MOMENT$_{\texttt{large}}$.
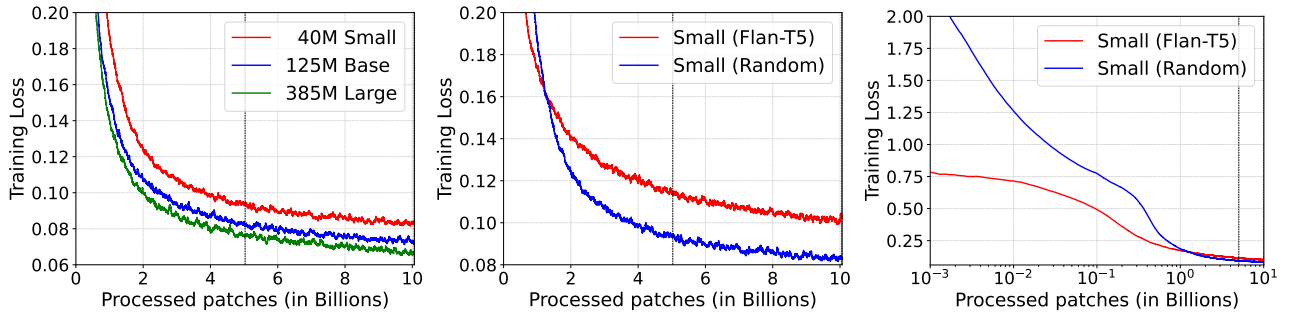
Figure 12. **Training losses (MSE).** A dashed vertical line denotes the first epoch. All models were trained with a batch size of 131072 patches. (*left*) Larger models obtain lower training loss. *right* Eventually, randomly initialized MOMENT-small outperform the same model initialized with Flan-T5 weights. The figure on the right is in log scale.

Model	ETTh1-96		
	Total Param. (M)	Trainable Param. (M)	Mem. (MiB)
MOMENT	347.53	6.29	2079
GPT4TS	82.28	1.12	1031
TimesNet	0.89	0.89	683
Time-LLM	3623.71	254.37	4537

Table 33. Efficiency analysis of MOMENT against other forecasting models on the ETTh1 with prediction horizon set to 96. MOMENT outperforms all the listed models and has a fraction of parameters as the most recent LLM-based forecasting method.

Sub-domain	Indicator	MOMENT
	Data size	1
	Data sources	1
	Data creators	0
	Data source selection	1
Data	Data curation	1
	Data augmentation	1
	Harmful data filtration	0
	Copyrighted data	1
	Data license	1
	Personal information in data	1
	Use of human labor	1
	Employment of data laborers	1
	Geographic distribution of data laborers	1
Data Labor	Wages	1
	Instructions for creating data	1
	Labor protections	1
	Third party partners	1
Data Access	Queryable external data access	1
	Direct external data access	1
	Compute usage	1
	Development duration	1
	Compute hardware	1
Compute	Hardware owner	1
	Energy usage	1
	Carbon emissions	1
	Broader environmental impact	0
	Model stages	1
Methods	Model objectives	1
	Core frameworks	1
	Additional dependencies	1
Data Mitigations	Mitigations for privacy	0
	Mitigations for copyright	0
	Upstream Subtotal	75%

Sub-domain	Indicator	MOMENT
	Input modality	1
	Output modality	1
Model Basics	Model components	1
	Model size	1
	Model architecture	1
	Centralized model documentation	1
	External model access protocol	1
Model Access	Blackbox external model access	1
	Full external model access	1
	Capabilities description	1
	Capabilities demonstration	1
Capabilities	Evaluation of capabilities	1
	External reproducibility of capabilities evaluation	0
	Third party capabilities evaluation	0
	Limitations description	1
Limitations	Limitations demonstration	1
	Third party evaluation of limitations	0
	Risks description	1
	Risks demonstration	0
	Unintentional harm evaluation	0
Risks	External reproducibility of unintentional harm evaluation	0
	Intentional harm evaluation	0
	External reproducibility of intentional harm evaluation	0
	Third party risks evaluation	0
Model Mitigations	Mitigations description	0
	Mitigations demonstration	0
	Mitigations evaluation	0
Mitigations	External reproducibility of mitigations evaluation	0
	Third party mitigations evaluation	0
Trustworthiness	Trustworthiness evaluation	0
	External reproducibility of trustworthiness evaluation	0
Inference	Inference duration evaluation	1
	Inference compute evaluation	1
	Model Subtotal	51.5%

Table 34. Expected (*left*) upstream and (*right*) model transparency scores. MOMENT has one of the highest upstream transparency. Our model transparency scores are lower due to (third-party) harm, mitigations, trustworthiness evaluation, which are not well understood for time series modeling.

Task	Method	Type	Reimplementation/ Rerun	Source
Long-horizon Forecasting	Time-LLM	LLM-based	✓	Time-LLM
	GPT4TS		×	One Fits All
	PatchTST, Fedformer, Autoformer, Stationary, ETSformer, LightTS, Informer, Reformer	Transformer-based	×	One Fits All
	Pyraformer, LogTrans		×	TimesNet
	TimesNet, DLinear	Deep learning	×	One Fits All
	N-BEATS		✓	N-BEATS
Short-horizon Forecasting	GPT4TS	LLM-based	✓	One Fits All
	TimesNet	Deep learning	✓	TimesNet
	N-BEATS		✓	N-BEATS
	AutoARIMA, AutoTheta, AutoETS, Seasonal Naive, Naive, Random Walk	Statistical learning	✓	Nixtla Statsforecast Repository
Classification	GPT4TS	LLM-based	✓	One Fits All
	TimesNet	Deep learning	✓	TimesNet
	TS2Vec, T-Loss, TNC, TS-TCC, TST	Unsupervised Representation learning	×	TS2Vec
	CNN, Encoder, FCN, MCNN, MLP, ResNet, t-LeNet, TWIESN	Deep learning	×	DL4TSC Repository
	DTW	Statistical learning	×	TS2Vec
Anomaly Detection	GPT4TS	LLM-based	✓	One Fits All
	TimesNet	Deep learning	✓	TimesNet
	Anomaly Transformer	Transformer-based	✓	Anomaly Transformer
	DGHL	Deep learning	✓	Time Series Model Selection
	k-NN	Statistical learning	✓	Time Series Model Selection
Imputation	GPT4TS	LLM-based	✓	One Fits All
	TimesNet	Deep learning	✓	TimesNet
	PatchTST, ETSformer, LightTS, Fedformer,Stationary, Autoformer, Informer, Reformer	Transformer-based	×	One Fits All
	DLinear	Deep learning	×	One Fits All
	Naive	Statistical learning	✓	Pandas FFill, Pandas BFill
	Linear, Nearest, Cubic		✓	Scipy Interp1D

Table 35. Source for the results for each baseline for all downstream task.